

## Durham Research Online

---

### Deposited in DRO:

12 March 2015

### Version of attached file:

Accepted Version

### Peer-review status of attached file:

Peer-reviewed

### Citation for published item:

Oerthel, M.-C. and Yufit, D.S. and Fox, M.A. and Bryce, M.R. and Low, P.J. (2015) 'Syntheses and structures of buta-1,3-diynyl complexes from 'on complex' cross-coupling reactions.', *Organometallics*, 34 (11). pp. 2395-2405.

### Further information on publisher's website:

<http://dx.doi.org/10.1021/om501186c>

### Publisher's copyright statement:

This document is the Accepted Manuscript version of a Published Work that appeared in final form in *Organometallics*, copyright © 2015 American Chemical Society after peer review and technical editing by the publisher. To access the final edited and published work see <http://dx.doi.org/10.1021/om501186c>.

### Additional information:

---

### Use policy

The full-text may be used and/or reproduced, and given to third parties in any format or medium, without prior permission or charge, for personal research or study, educational, or not-for-profit purposes provided that:

- a full bibliographic reference is made to the original source
- a [link](#) is made to the metadata record in DRO
- the full-text is not changed in any way

The full-text must not be sold in any format or medium without the formal permission of the copyright holders.

Please consult the [full DRO policy](#) for further details.

This document is confidential and is proprietary to the American Chemical Society and its authors. Do not copy or disclose without written permission. If you have received this item in error, notify the sender and delete all copies.

**Syntheses and Structures of Buta-1,3-Diynyl Complexes  
from 'On Complex' Cross-Coupling Reactions**

|                               |  |
|-------------------------------|--|
| Journal:                      | <i>Organometallics</i>   |
| Manuscript ID:                | om-2014-01186c.R1  |
| Manuscript Type:              | Article  |
| Date Submitted by the Author: | 01-Feb-2015  |
| Complete List of Authors:     | Oerthel, Marie-Christine; Durham University, Department of Chemistry<br>Yufit, Dmitry; University of Durham, Chemistry<br>Fox, Mark; University of Durham, Department of Chemistry<br>Bryce, Martin; University of Durham, Chemistry<br>Low, Paul; University of Western Australia, School of Chemistry and Biochemistry |
|                               |  |

SCHOLARONE™  
Manuscripts

# Syntheses and Structures of Buta-1,3-Diynyl Complexes from ‘On Complex’ Cross-Coupling Reactions

Marie-Christine Oerthel,<sup>†</sup> Dmitry S. Yufit,<sup>†</sup> Mark A. Fox,<sup>†</sup> Martin R. Bryce,<sup>\*†</sup> Paul J. Low<sup>\*‡</sup>

<sup>†</sup> Department of Chemistry, Durham University, South Rd, Durham, DH1 3LE, UK

<sup>‡</sup> School of Chemistry and Biochemistry, University of Western Australia, 35 Stirling Highway, Crawley, Perth 6009, Australia

Email: [m.r.bryce@durham.ac.uk](mailto:m.r.bryce@durham.ac.uk), [paul.low@uwa.edu.au](mailto:paul.low@uwa.edu.au)

## ABSTRACT

The Pd(PPh<sub>3</sub>)<sub>4</sub> / CuI co-catalyzed reaction of Ru(C≡CC≡CH)(PPh<sub>3</sub>)<sub>2</sub>Cp (**2**) with aryl iodides, Ar-I (**3** Ar = C<sub>6</sub>H<sub>4</sub>CN-4 (**a**); C<sub>6</sub>H<sub>4</sub>Me-4 (**b**); C<sub>6</sub>H<sub>4</sub>OMe-4 (**c**); 2,3-dihydrobenzo[*b*]thiophene (**d**); C<sub>5</sub>H<sub>4</sub>N (**e**)) proceeds smoothly in diisopropylamine and under an inert atmosphere to give the substituted buta-1,3-diynyl complexes Ru(C≡CC≡CAr)(PPh<sub>3</sub>)<sub>2</sub>Cp (**4a - e**) in moderate to good yield. The procedure allows the rapid preparation of a range of metal complexes of arylbuta-1,3-diynyl ligands without necessitating the prior synthesis of the individual buta-1,3-diyne as ligand precursors. Similar reaction of **2** with half an equivalent of 1,4-diiodobenzene affords the bimetallic derivative {Ru(PPh<sub>3</sub>)<sub>2</sub>Cp}<sub>2</sub>(μ-C≡CC≡C-1,4-C<sub>6</sub>H<sub>4</sub>-C≡CC≡C) (**5**). In the presence of atmospheric oxygen, homocoupling of the diynyl reagent **2** takes place to provide the

octa-1,3,5,7-tetrayndiyl complex  $\{\text{Ru}(\text{PPh}_3)_2\text{Cp}\}_2(\mu\text{-C}\equiv\text{CC}\equiv\text{CC}\equiv\text{CC}\equiv\text{C})$  (**6**).

Crystallographically determined molecular structures are reported for five complexes (**4a**, **4b**, **4d**, **5** and **6**). Quantum chemical calculations indicate that the HOMOs are mainly located on the  $\text{C}_4\text{-C}_6\text{H}_4\text{-C}_4$  and  $\text{C}_8$  bridges for **5** and **6** respectively, whilst spectroelectrochemical (UV-vis-NIR and IR) studies on **6** establish that oxidation takes place at the  $\text{C}_8$  bridge, likely followed by cyclodimerization reactions of the bridging ligand.

## INTRODUCTION

Metal oligo/polyynyl  $\text{M}\{(\text{C}\equiv\text{C})_n\text{H}\}\text{L}_x$  species have attracted significant interest over several decades, serving as scaffolds for the assembly of bi-<sup>1-13</sup> and poly-metallic<sup>14-26</sup> complexes, and as models and building blocks for metallomacrocycles,<sup>15, 27-29</sup> and metallo-polymers.<sup>30-35</sup> Detailed studies of the underlying electronic structure of this family of complexes have been undertaken, using a variety of computational and spectroscopic methods, often with a view to modelling the behavior of these prototypical molecular wires.<sup>21,36-39</sup> The terminal  $\text{C}\equiv\text{CH}$  moiety in polyynyl complexes  $\text{M}\{(\text{C}\equiv\text{C})_{n-1}\text{C}\equiv\text{CH}\}\text{L}_x$  offers a convenient entry point for the preparation of a wide range of polyynyl derivatives; however, the functionalization reactions of  $-(\text{C}\equiv\text{C})_{n-1}\text{C}\equiv\text{CH}$  ligands are largely based on deprotonation and subsequent trapping with various electrophiles,<sup>9,40-44</sup> including metal complex electrophiles.<sup>45,46</sup>

To the best of our knowledge, the use of the Sonogashira cross-coupling reaction as a tool to prepare substituted derivatives of buta-1,3-diyl complexes was first demonstrated in

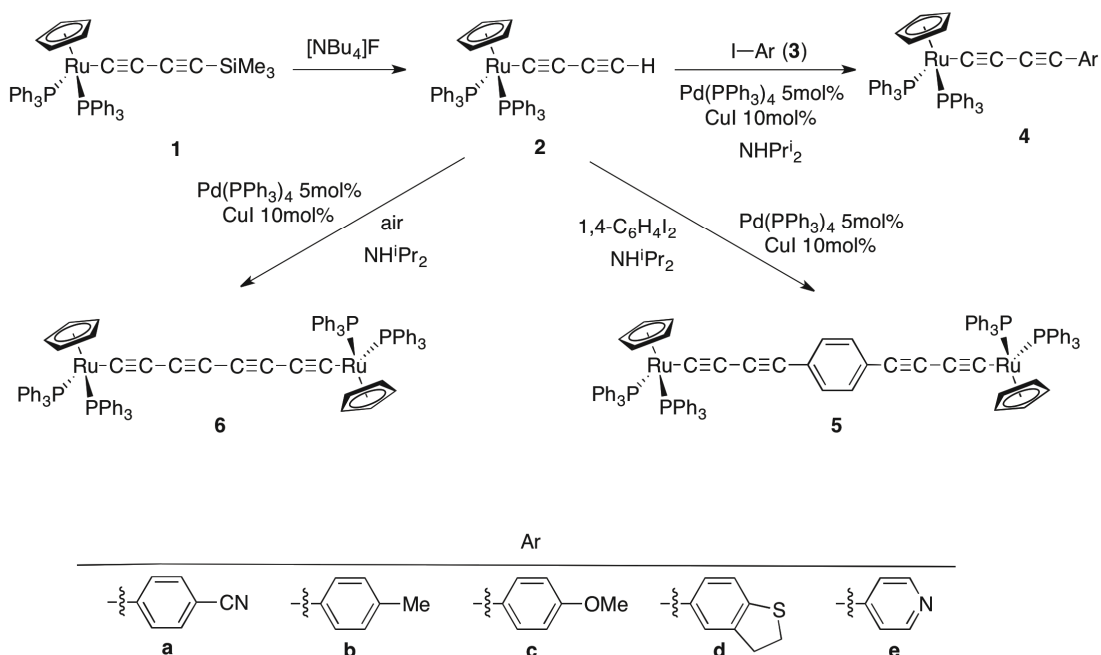


1  
2  
3 reactions of  $W(C\equiv CC\equiv CH)(CO)_3Cp$  with iodoaromatics.<sup>47</sup> However, despite further  
4  
5 successful demonstrations of this ‘chemistry on the complex’ concept to functionalize<sup>48-52</sup>  
6  
7 or extend<sup>53-64</sup> metal-alkynyl ligands through homo or cross-coupling protocols, the use of  
8  
9 cross-coupling reactions to functionalize metal complexes<sup>65</sup> has been largely overlooked  
10  
11 for the preparation of more functional metal alkynyl complexes. More conventional  
12  
13 strategies involving the metallation of pre-formed alkynes and (poly)ynes of general form  
14  
15  $H(C\equiv C)_{n-1}C\equiv CR$  or  $Me_3Si(C\equiv C)_{n-1}C\equiv CR$ <sup>8,66-69</sup> have been preferred.  
16  
17  
18  
19  
20  
21  
22

23 We now report the use of Sonogashira-style cross-coupling reactions in the preparation of  
24  
25 a range of ruthenium buta-1,3-diynyl complexes from a common  
26  
27  $Ru(C\equiv CC\equiv CH)(PPh_3)_2Cp$  platform. This strategy obviates the need to prepare different  
28  
29 diyne ligands for each and every complex, providing rapid access to a range of  
30  
31 complexes with various aryl buta-1,3-diynyl ligands.  
32  
33  
34  
35  
36  
37  
38

## 39 RESULTS AND DISCUSSION

40  
41 Fluoride-induced desilylation of the readily-available complex  
42  
43  $Ru(C\equiv CC\equiv CSiMe_3)(PPh_3)_2Cp$  (**1**) affords the terminal buta-1,3-diyl complex  
44  
45  $Ru(C\equiv CC\equiv CH)(PPh_3)_2Cp$  (**2**),<sup>18</sup> which was chosen as a suitable platform on which to test  
46  
47 Sonogashira cross-coupling reactions with a wider range of aryl iodides **3** than explored  
48  
49 previously on the  $W(C\equiv CC\equiv CH)(CO)_3Cp$  platform (Scheme 1).<sup>47</sup>  
50  
51  
52  
53  
54  
55  
56  
57  
58  
59  
60



**Scheme 1.** The Sonogashira cross-coupling reactions of **2** with aryl iodides **3a - e** yielding **4a - e**, and related syntheses of **5** and **6**.

Reaction of **2** with the aryl iodides **3a-e** in diisopropylamine co-catalyzed by a simple  $\text{Pd(PPh}_3)_4$  (5 mol%) /  $\text{CuI}$  (10 mol%) mixture gave the substituted buta-1,3-diynyl complexes  $\text{Ru(C}\equiv\text{CC}\equiv\text{CAr)(PPh}_3)_2\text{Cp}$  **4a - e** in moderate (**4a**, 47%; **4c**, 59%; **4d**, 54%; **4e**, 60%) to good (**4b**, 87%) yields. These examples illustrate the versatility of the ‘chemistry-on-complex’ strategy; through this approach buta-1,3-diynyl complexes with electron-withdrawing (**3a**  $\text{C}_6\text{H}_4\text{CN}$ ), electro-neutral (**3b**  $\text{C}_6\text{H}_4\text{Me}$ ), electron-donating (**3c**  $\text{C}_6\text{H}_4\text{OMe}$ ) or metal surface contacting (**3d** 2,3-dihydrobenzo[*b*]thiophene (DHBT); **3e**  $\text{C}_5\text{H}_4\text{N}$ ) substituents have been obtained. Similarly, reaction of **2** with one-half equivalent of 1,4-diiodobenzene gave the bimetallic bis(butadiynyl) complex  $\{\text{Ru(PPh}_3)_2\text{Cp}\}_2(\mu\text{-C}\equiv\text{CC}\equiv\text{C-1,4-C}_6\text{H}_4\text{C}\equiv\text{CC}\equiv\text{C})$  (**5**) in 67% yield.

The products were obtained in good purity as precipitates from the reaction mixtures and, where necessary, further purification was achieved by column chromatography and / or crystallization. Identification of the products was readily achieved through a combination of IR,  $^1\text{H}$ ,  $^{13}\text{C}$  and  $^{31}\text{P}$  NMR spectroscopies, MALDI-TOF and high-resolution ES mass spectrometry. The phosphine ligands were detected in the  $^{31}\text{P}$  NMR spectra as singlets in the narrow range 48.2 (**4a**) - 49.1 (**4c**) ppm, whilst the Cp ligands were detected in the  $^1\text{H}$  spectra between 4.33 - 4.38 ppm. The  $^{13}\text{C}$  NMR resonances were assigned with aid of values obtained from calculations modeled on **4a**. In all cases the buta-1,3-diynyl ligand gave rise to a two-band  $\nu(\text{C}\equiv\text{CC}\equiv\text{C}\text{Ar})$  pattern with absorptions near 2160 and 2020  $\text{cm}^{-1}$  that can be approximated as the local oscillations of the  $\text{C}\equiv\text{C}\text{Ar}$  and  $\text{Ru}-\text{C}\equiv\text{C}$  fragments, respectively.<sup>70</sup> In each case the MALDI-TOF spectrum contained the molecular ion, together with a fragment ion derived from loss of  $\text{PPh}_3$  in some cases.

Although most commonly used as a cross-coupling methodology, it is well-known that the Sonogashira cycle can be intercepted by oxidants to promote homo-coupling of the terminal alkyne.<sup>71-74</sup> Indeed, Sonogashira-like conditions in the presence of an additional oxidant are emerging as a viable alternative to the Glaser-Hay type methods of 1,3-diyne synthesis.<sup>75</sup> Accordingly, the reaction of **2** with catalytic  $\text{Pd}(\text{PPh}_3)_4$  /  $\text{CuI}$  in  $\text{NHPr}_2^i$  in an open flask proceeded rapidly to give the homo-coupled octa-1,3,5,7-tetrayndiyl complex  $\{\text{Ru}(\text{PPh}_3)_2\text{Cp}\}_2(\mu\text{-C}\equiv\text{CC}\equiv\text{CC}\equiv\text{CC}\equiv\text{C})$  (**6**, 55%). Complex **6** (60%)<sup>76</sup> and the closely related buta-1,3-diyniyl  $\{\text{Ru}(\text{PPh}_3)_2\text{Cp}\}_2(\mu\text{-C}\equiv\text{CC}\equiv\text{C})$  and hexa-1,3,5-

triyndiyl{Ru(PPh<sub>3</sub>)<sub>2</sub>Cp}<sub>2</sub>(μ-C≡CC≡CC≡C)<sup>77</sup> complexes have previously been prepared from desilylation / metallation reactions of the appropriate di-, tri- or tetra-yne Me<sub>3</sub>Si-(C≡C)<sub>n</sub>-SiMe<sub>3</sub> with RuCl(PPh<sub>3</sub>)<sub>2</sub>Cp in presence of KF. Other octa-1,3,5,7-tetrayndiyl complexes have been prepared from oxidative Hay or Glaser style coupling of buta-1,3-diynyl complexes,<sup>2,58,60,78-82</sup> and the approach described here provides a complementary, and highly convenient route to these systems.

*Molecular Structures.* Single crystals suitable for X-ray diffraction analysis were obtained for the buta-1,3-diynyl complexes **4a**, **4b**, **4d** and bimetallic complexes **5**•CH<sub>2</sub>Cl<sub>2</sub> and **6**•2CH<sub>2</sub>Cl<sub>2</sub>; the structure of **6**•4CHCl<sub>3</sub> has been reported recently by Bruce and colleagues.<sup>82</sup> Representative plots of **4a**, **5**•CH<sub>2</sub>Cl<sub>2</sub> and **6**•2CH<sub>2</sub>Cl<sub>2</sub> showing the atom labeling scheme are given in Figures 1 - 3, and selected bond lengths and angles for **4a**, **4b**, **4d**, **5**•CH<sub>2</sub>Cl<sub>2</sub>, **6**•2CH<sub>2</sub>Cl<sub>2</sub> are summarized in Table 1 together with data from **6**•4CHCl<sub>3</sub><sup>82</sup> and DFT optimized structures (vide infra). The diynyl complexes **4a**, **4b** and **4d** featuring the Ru(PPh<sub>3</sub>)<sub>2</sub>Cp fragment display bond lengths associated with both the diynyl ligand and the metallic half-sandwich moiety that barely differ from the few other examples of Ru(C≡CC≡CR)(PPh<sub>3</sub>)<sub>2</sub>Cp compounds reported to date: (R = SiMe<sub>3</sub>,<sup>18</sup> C(Ph)CBr<sub>2</sub>,<sup>69</sup> Ph,<sup>77</sup> and CN<sup>83</sup>). Thus, the ruthenium centers have the usual pseudo-octahedral geometry, with bond lengths and angles in the ranges: Ru-P 2.284(1) – 2.342(2) Å and P(1)-Ru-P(2) 96.42(8) – 101.39(1)°, P(1,2)-Ru-C(1) 88.37(6) - 92.24(5)°. The Ru-C(1) lengths fall between 1.984(2) Å (**4a**) and 2.002(3) Å (**4b**) which compares with the 1.986(4) - 1.99(1) Å range found in previous examples. For the diynyl chain, the bond lengths display the expected pattern of short-long alternation: C(1)-C(2) 1.21(1) -

1.23(1) Å; C(2)-C(3) 1.35(1) - 1.38(1) Å; C(3)-C(4) 1.168(14) - 1.216(4) Å; and the chain is essentially linear, with angles: Ru-C(1)-C(2) 172.8(2) - 175.6(3)°; C(1)-C(2)-C(3) 170(1) - 178(1)°.

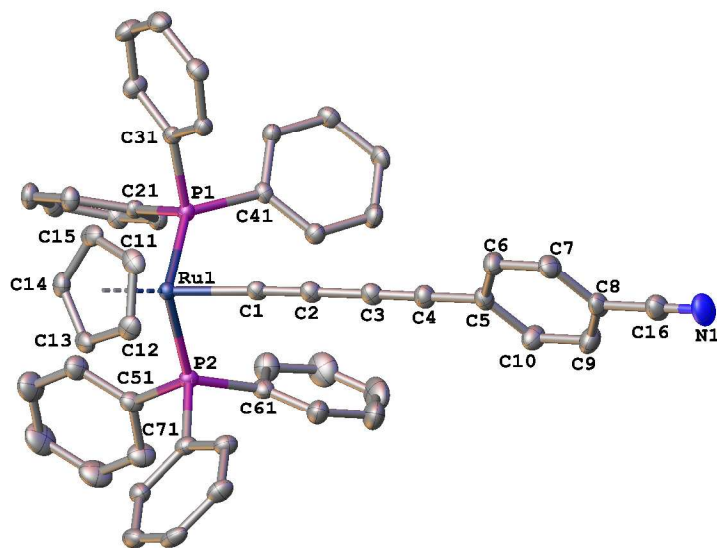


Fig.1 Molecular structure of **4a** showing the atom labeling scheme. In this and all subsequent plots thermal ellipsoids are drawn at 50% probability level, H-atoms and solvent molecules (when present) are omitted for clarity.

Table 1. Selected crystallographically determined bond lengths (Å) and angles (°) for complexes **4a**, **4b**, **4d**, **5**•CH<sub>2</sub>Cl<sub>2</sub> and **6**•2CH<sub>2</sub>Cl<sub>2</sub>, with related data from **6**•4CHCl<sub>3</sub> and DFT optimized (B3LYP/3-21G\*/CPCM-CH<sub>2</sub>Cl<sub>2</sub>) geometries (**4a'**, **5'** and **6'**)

| Bond lengths (Å)               | <b>4a</b> | <b>4a'</b> | <b>4b</b> | <b>4d</b>   | <b>5</b> •CH <sub>2</sub> Cl <sub>2</sub> | <b>5'</b>      | <b>6</b> •2CH <sub>2</sub> Cl <sub>2</sub> | <b>6</b> •4CHCl <sub>3</sub> <sup>82</sup> | <b>6'</b>      |
|--------------------------------|-----------|------------|-----------|-------------|---|----------------|--|--|----------------|
| Ru-P(1)                        | 2.2936(5) | 2.3366     | 2.2884(8) | 2.2844 (5)  | 2.342(2)                                  | 2.3324, 2.3344 | 2.298(2)                                   | 2.305(2)                                   | 2.3432, 2.3432 |
| Ru-P(2)                        | 2.2915(5) | 2.3315     | 2.3001(7) | 2.3088 (5)  | 2.306(3)                                  | 2.3245, 2.3233 | 2.282(2)                                   | 2.291(2)                                   | 2.3404, 2.3314 |
| Ru-C(1)                        | 1.984(2)  | 1.9783     | 2.002(3)  | 1.9947 (19) | 1.965(10)                                 | 1.9855, 1.9860 | 1.976(5)                                   | 1.963(6)                                   | 1.9822, 1.9841 |
| C(1)-C(2)                      | 1.221(3)  | 1.2420     | 1.214(4)  | 1.226 (3)   | 1.233(13)                                 | 1.2406, 1.2407 | 1.229(7)                                   | 1.237(7)                                   | 1.2440, 1.2445 |
| C(2)-C(3)                      | 1.371(3)  | 1.3485     | 1.380(4)  | 1.373 (3)   | 1.346(14)                                 | 1.3519, 1.3519 | 1.362(8)                                   | 1.370(8)                                   | 1.3445, 1.3444 |
| C(3)-C(4)                      | 1.204(3)  | 1.2255     | 1.216(4)  | 1.211 (3)   | 1.168(14)                                 | 1.2250, 1.2250 | 1.220(7)                                   | 1.197(7)                                   | 1.2345, 1.2346 |
| C(4)-C(5) / C(4)-C(4')         | 1.430(3)  | 1.4139     | 1.429(4)  | 1.431 (3)   | 1.476(16)                                 | 1.4174, 1.4175 | 1.358(11)                                  | 1.385(12)                                  | 1.3395         |
| Angles (°)                     |           |            |           |             |   |                |  |  |                |
| P(1)-Ru-P(2)                   | 101.39(2) | 102.63     | 98.89(3)  | 97.44(2)    | 96.42(8)                                  | 101.07, 101.23 | 100.27(5)                                  | 98.74(4)                                   | 101.95, 100.35 |
| P(1)-Ru-C(1)                   | 90.67(5)  | 90.96      | 89.89(9)  | 92.24(5)    | 93.9(3)                                   | 91.07, 91.46   | 86.49(15)                                  | 87.2(1)                                    | 88.35, 92.20   |
| P(2)-Ru-C(1)                   | 88.37(6)  | 88.24      | 91.77(8)  | 91.85(5)    | 90.1(3)                                   | 91.13, 90.71   | 94.12(16)                                  | 93.5(1)                                    | 92.07, 89.76   |
| Ru-C(1)-C(2)                   | 175.0(2)  | 175.10     | 175.6(3)  | 172.8(2)    | 172.8(8)                                  | 173.91, 173.86 | 168.5(5)                                   | 174.6(4)                                   | 173.17, 175.94 |
| C(1)-C(2)-C(3)                 | 178.6(2)  | 179.21     | 173.5(3)  | 174.9(2)    | 170.3(12)                                 | 178.95, 179.03 | 170.3(6)                                   | 173.6(5)                                   | 178.35, 178.76 |
| C(2)-C(3)-C(4)                 | 178.3(2)  | 179.63     | 177.9(3)  | 178.2(2)    | 176.2(12)                                 | 179.24, 179.87 | 175.0(6)                                   | 176.7(5)                                   | 178.97, 179.08 |
| C(3)-C(4)-C(5)/C(3)-C(4)-C(4') | 173.4(2)  | 179.63     | 173.6(3)  | 179.4(2)    | 177.2(13)                                 | 179.11, 179.35 | 179.8(8)                                   | 178.3(7)                                   | 179.05         |

In the solid state, the bimetallic complexes **5**•CH<sub>2</sub>Cl<sub>2</sub> and **6**•2CH<sub>2</sub>Cl<sub>2</sub> adopt a *trans*-conformation of the Cp rings. The torsion angle C(0)-Ru-C(5)-C(6) is 172.9(9)° (C(0) is the centroid of the Cp ring) suggesting that, at least in the structure adopted in the solid state, the d<sub>yz</sub> and d<sub>xz</sub> orbitals of the Ru atom are able to participate in conjugation along the carbon-rich bridging ligand. The octa-1,3,5,7-tetrayn-1,8-diyl ligand in **6**•2CH<sub>2</sub>Cl<sub>2</sub> displays the sigmoidal distortions from linearity often observed for extended carbon chain complexes.<sup>82,84</sup> In **5**•CH<sub>2</sub>Cl<sub>2</sub> the Ru-C(1) distance (1.965(10) Å) is the shortest in the series, and arguably shorter than the Ru-C<sub>α</sub> bond found in the related hexa-1,3,5-triyn-1,6-diyl complex [{Ru(PPh<sub>3</sub>)<sub>2</sub>Cp}<sub>2</sub>(μ-C≡CC≡CC≡C)] (2.001(6) Å),<sup>77</sup> and in **6**•2CH<sub>2</sub>Cl<sub>2</sub>, but equal to that found in **6**•4CHCl<sub>3</sub> (1.963(6) Å).<sup>82</sup> Clearly, these small structural variations must be treated cautiously to avoid over-interpretation.

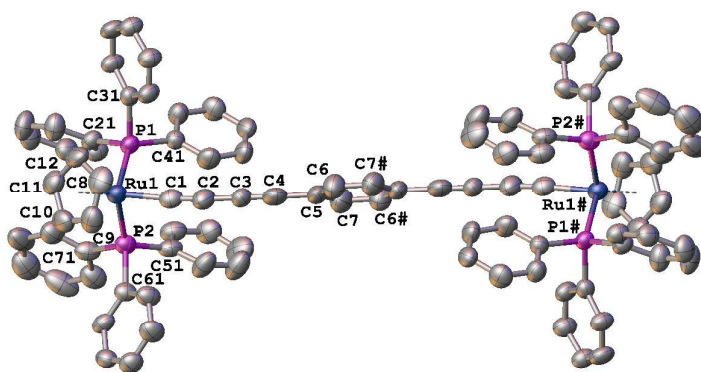


Fig. 2. A plot of a molecule of **5**•CH<sub>2</sub>Cl<sub>2</sub>. The molecule is located in the center of symmetry.

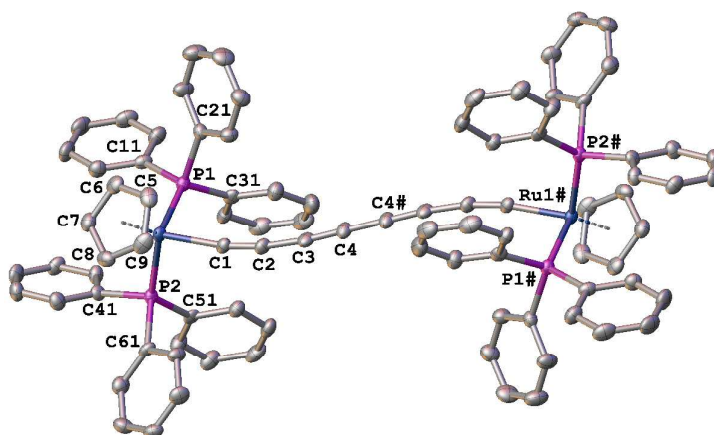


Fig. 3. A plot of a molecule of **6**•2CH<sub>2</sub>Cl<sub>2</sub>. The molecule is located in the center of symmetry.

### Electrochemistry

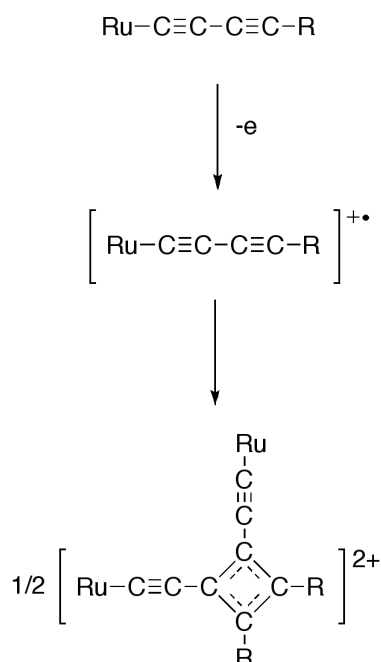
The monometallic complexes **4a-4e** each give one oxidation wave that is electrochemically reversible but chemically irreversible, supported by the observation of a 30 mV shift in the peak potential per decade change in scan rate, and peak currents linear vs  $v^{1/2}$ , with peak potentials at 100 mV/s that vary between 0.06 V-0.22 V and exhibit a trend in accord with the electronic character of the aryl substituent: Ru(C≡CC≡CC<sub>6</sub>H<sub>4</sub>OMe-4)(PPh<sub>3</sub>)<sub>2</sub>Cp **4c** < Ru(C≡CC≡CC<sub>6</sub>H<sub>4</sub>Me-4)(PPh<sub>3</sub>)<sub>2</sub>Cp **4b** < Ru(C≡CC≡CDHBT)(PPh<sub>3</sub>)<sub>2</sub>Cp **4d** < Ru(C≡CC≡CC<sub>6</sub>H<sub>4</sub>CN-4)(PPh<sub>3</sub>)<sub>2</sub>Cp **4a** < Ru(C≡CC≡CC<sub>3</sub>H<sub>4</sub>N)(PPh<sub>3</sub>)<sub>2</sub>Cp **4e** (Table 2). The irreversibility of similar diynyl complexes has been noted on previous occasions,<sup>18</sup> and is likely due to intermolecular coupling of the generated diynyl radicals.<sup>66,85</sup> A general scheme on this oxidation dimerization process is depicted in Scheme 2.



Table 2. Electrochemical data of the Ru(C≡CC≡C-Ar)(PPh<sub>3</sub>)<sub>2</sub>Cp derivatives **4a-e**, **5**, and **6**.<sup>a</sup>

| Compound   | <i>E</i> <sub>pa</sub> (1)  | <i>E</i> <sub>pa</sub> (2) | <i>E</i> <sub>pa</sub> (3) | <i>E</i> <sub>pa</sub> (4) |
|--|-----------------------------|----------------------------|----------------------------|----------------------------|
| Ru(C≡CC≡CC <sub>6</sub> H <sub>4</sub> OMe-4)(PPh <sub>3</sub> ) <sub>2</sub> Cp <b>4c</b>                   | 0.06                        |                            |                            |                            |
| Ru(C≡CC≡CC <sub>6</sub> H <sub>4</sub> Me-4)(PPh <sub>3</sub> ) <sub>2</sub> Cp <b>4b</b>                    | 0.09                        |                            |                            |                            |
| Ru(C≡CC≡CDHBT)(PPh <sub>3</sub> ) <sub>2</sub> Cp <b>4d</b>  | 0.11                        |                            |                            |                            |
| Ru(C≡CC≡CC <sub>6</sub> H <sub>4</sub> CN-4)(PPh <sub>3</sub> ) <sub>2</sub> Cp <b>4a</b>                    | 0.21                        |                            |                            |                            |
| Ru(C≡CC≡CC <sub>5</sub> H <sub>4</sub> N)(PPh <sub>3</sub> ) <sub>2</sub> Cp <b>4e</b>                       | 0.22                        |                            |                            |                            |
| {Ru(PPh <sub>3</sub> ) <sub>2</sub> Cp} <sub>2</sub> (μ-C≡CC≡CC <sub>6</sub> H <sub>5</sub> C≡CC≡C) <b>5</b> | 0.04                        | 0.24                       |                            |                            |
|  | <i>E</i> <sub>1/2</sub> (1) | <i>E</i> <sub>pa</sub> (2) | <i>E</i> <sub>pa</sub> (3) | <i>E</i> <sub>pa</sub> (4) |
| {Ru(PPh <sub>3</sub> ) <sub>2</sub> Cp} <sub>2</sub> (μ-C≡CC≡CC≡CC≡C) <b>6</b>                               | -0.16                       | 0.15                       | 0.61                       | 0.82                       |

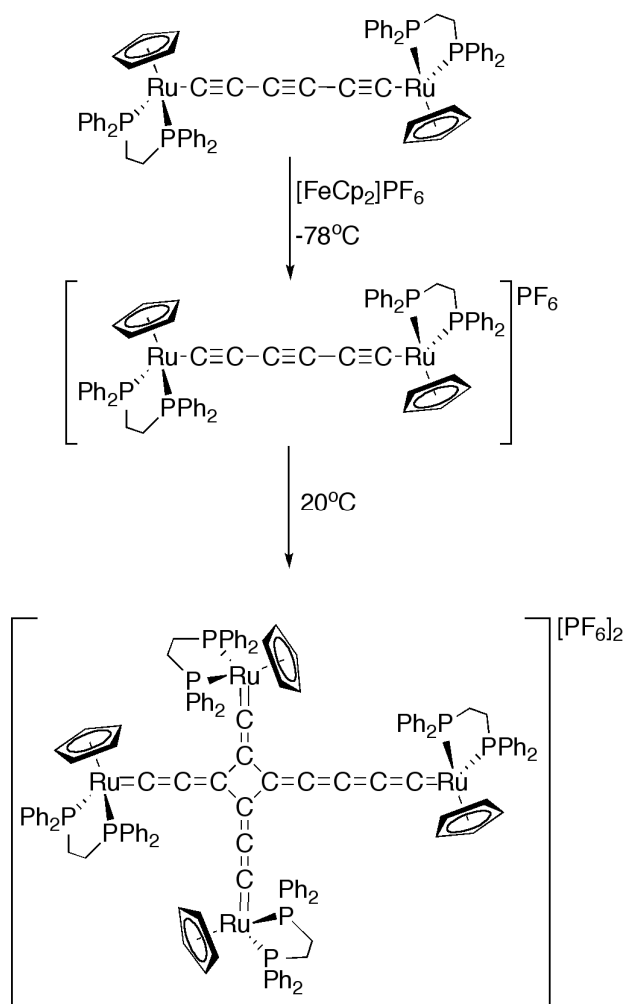
<sup>a</sup> *E*<sub>pa</sub> (anodic peak potential, V) vs. ferrocene/ferrocenium (FeCp<sub>2</sub>/[FeCp<sub>2</sub>]<sup>+</sup> = 0 V) (CH<sub>2</sub>Cl<sub>2</sub>, 0.1 M NBu<sub>4</sub>PF<sub>6</sub>, Pt dot working electrode). Data recorded against an internal decamethylferrocene/ decamethylferrocenium (FeCp\*<sub>2</sub>/[FeCp\*<sub>2</sub>]<sup>+</sup>) standard. Under these conditions FeCp\*<sub>2</sub>/[FeCp\*<sub>2</sub>]<sup>+</sup> = -0.53 V vs FeCp<sub>2</sub>/[FeCp<sub>2</sub>]<sup>+</sup>.



**Scheme 2.** A general oxidation and dimerization process for a  $\text{Ru}-\text{C}\equiv\text{C}-\text{C}\equiv\text{C}-\text{R}$  complex  $[\text{Ru} = \text{Ru}(\text{PP})\text{Cp}']$  where  $\text{PP} = (\text{PPh}_3)_2$  or  $\text{dppe}$ ,  $\text{Cp}' = \text{Cp}$  or  $\text{Cp}^*$ ;  $\text{R} = \text{aryl}$  or  $-(\text{C}\equiv\text{C})_n-\text{Ru}$ .

Similarly, two electrochemically reversible, but chemically irreversible, oxidation waves (peak potential displaying 30 mV shift per decade change in scan rate, peak currents linear vs  $v^{1/2}$ ) are observed in the cyclic voltammogram of the bis(butadiynyl) complex **5** (Table 2). The chemical stability of  $[\mathbf{5}]^+$  did not improve at lower temperatures (ambient to  $-30\text{ }^\circ\text{C}$ ) and chemical complications evidenced by the appearance of a new reduction wave at  $-0.15\text{ V}$  on the return scan were still apparent at  $v = 800\text{ mV s}^{-1}$ . The chemical instability of this bis(butadiynyl) complex is entirely consistent with the limited chemical stability of **4a** – **4e**, and other related systems reported elsewhere.<sup>85</sup>

In contrast to these monometallic buta-1,3-diyndyl derivatives, the bimetallic octa-1,3,5,7-tetrayndiyl complex **6** displays one fully reversible oxidation wave ( $i_{pa}/i_{pc} = 0.98$ ,  $\Delta E_p = 74$  mV which is comparable with the internal decamethylferrocene reference) and three subsequent, irreversible processes (Table 2). These four processes correspond well to the four oxidation processes described for the analogous buta-1,3-diyndiyl ( $-C\equiv CC\equiv C-$ ) complex  $\{Ru(PPh_3)_2Cp\}_2(\mu-C\equiv CC\equiv C)$ .<sup>86,87</sup> In the case of the shorter chain analogue,  $\{Ru(PPh_3)_2Cp\}_2(\mu-C\equiv CC\equiv C)$ , the first three redox processes at least are chemically reversible. Spectroelectrochemical studies supported by quantum chemical calculations have been used to demonstrate the progressive shift in the character of the carbon chain from butadiyndiyl ( $-C\equiv CC\equiv C-$ ) through butatrienyliidene ( $=C=C=C=C=$ ) towards butynediylidide ( $\equiv CC\equiv CC\equiv$ ).<sup>86,87</sup> The cation  $[\{Ru(PPh_3)_2Cp\}_2(\mu-C\equiv CC\equiv C)]^+$  is sufficiently kinetically and thermodynamically stable to be isolated, and has been explored in a number of contexts.<sup>86,87</sup> The closely related hexa-1,3,5-triyn-1,6-diyl complex  $\{Ru(dppe)_2Cp\}_2(\mu-C\equiv CC\equiv CC\equiv C)$  exhibits three redox processes in the potential window explored, the first two of which were reversible, the third being only partially chemically reversible.<sup>68</sup> However, in contrast to the  $C_4$  example, the more exposed  $C_6$  chain in  $[\{Ru(dppe)_2Cp\}_2(\mu-C\equiv CC\equiv CC\equiv C)]^+$  undergoes an intermolecular coupling reaction on timescales longer than the voltammetric measurement at temperatures above  $-10$  °C to give an unusual dimeric complex featuring a cyclobutene motif formed by coupling between  $C_\alpha\equiv C_\beta$  of one molecule with  $C_\gamma\equiv C_\delta$  of another (Scheme 3).<sup>68</sup> This contrasting reactivity prompted further investigation of the first electrochemically reversible process observed for the  $C_8$  bridged complex **6** by spectroelectrochemical methods.

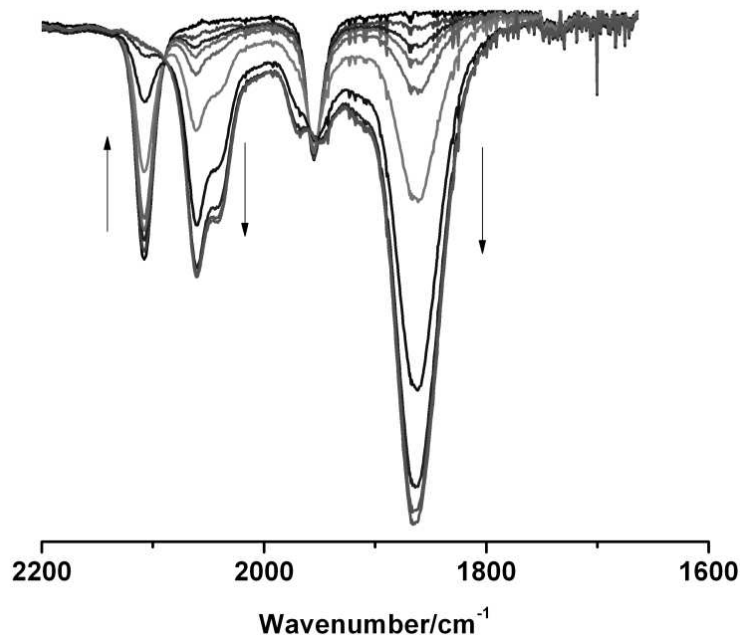


**Scheme 3.** The synthesis and dimerization of  $[\{\text{Ru}(\text{dppe})_2\text{Cp}\}_2(\mu\text{-C}\equiv\text{CC}\equiv\text{CC}\equiv\text{C})]^{+}$ .<sup>68</sup>

### Spectroelectrochemistry

Spectroelectrochemical (UV-vis-NIR, IR) studies of **6** were conducted in a Hartl-style OTTLE cell<sup>88</sup> in 0.1 M  $\text{NBu}_4\text{PF}_6$  /  $\text{CH}_2\text{Cl}_2$  solution at ambient temperature. The characteristic  $\nu(\text{C}\equiv\text{C})$  bands of **6** were observed at 2107 and 1955  $\text{cm}^{-1}$  in the IR spectrum. On oxidation of **6**, the spectrum evolved into a more complex series of  $\nu(\text{CC})$  bands between 2059 - 1862  $\text{cm}^{-1}$  with clear maxima at 2059 s, 2039 sh, 1953 m and 1862 vs  $\text{cm}^{-1}$  (Figure 4). However, back reduction failed to completely recover

As noted above, the oxidation of a related hexa-1,3,5-triyn-1,6-diyl complex  $[\{\text{Ru}(\text{dppe})\text{Cp}\}_2(\mu\text{-C}\equiv\text{CC}\equiv\text{CC}\equiv\text{C})]$  was reported<sup>68</sup> to give the dimerization product  $\{\text{cyclo-C}([\text{Ru})\text{C}(\text{CCCC}[\text{Ru})\text{C}(\text{CC})\text{Ru})\text{C}(\text{CC}[\text{Ru})])\}^{2+}$  ( $[\text{Ru}] = \text{Ru}(\text{dppe})\text{Cp}$ ) (Scheme 3). This dimer has a remarkably similar  $\nu(\text{C}\equiv\text{C})$  band pattern at 2080 - 1930  $\text{cm}^{-1}$  as for the oxidized product shown in Figure 4 and suggests that a dimerization product is also formed on oxidation of **6**.



The oxidation of **6** was also followed in the UV-vis-NIR region. Upon one-electron oxidation, the spectra display a loss of the intense UV band at 29793 cm<sup>-1</sup> and the

1  
2  
3 appearance of new features in the NIR region at  $7500\text{ cm}^{-1}$ , which grew and decayed  
4  
5 during the earlier stages of the electrolysis, and two further bands at 11048 and 14280  
6  
7  $\text{cm}^{-1}$ , which continued to grow throughout the experiment (Figure 5). Again, back-  
8  
9 reduction failed to regenerate **6**, confirming the EC process in the initial stages of the  
10  
11 spectroelectrochemical experiment.  
12  
13  
14  
15  
16  
17

18 Although we have not identified the product ultimately formed on oxidation of **6**, the  
19  
20 transient band observed at  $7500\text{ cm}^{-1}$  likely arises from the initial oxidation product  
21  
22  $[\mathbf{6}]^+$ , whilst the relatively intense, persistent features observed at the later stages at  
23  
24 11048 and  $14280\text{ cm}^{-1}$  are similar to those observed in the absorption spectrum of  
25  
26  $\{\text{cyclo-C}([\text{Ru}])\text{C}(\text{CCCC}[\text{Ru}])\text{C}(\text{CC}[\text{Ru}])\text{C}(\text{CC}[\text{Ru}])\}^{2+}$  ( $12060, 16640\text{ cm}^{-1}$ ,  $[\text{Ru}] =$   
27  
28  $\text{Ru}(\text{dppe})\text{Cp}$ , Scheme 3).<sup>68</sup> It therefore appears probable that the initial oxidation of **6**  
29  
30 to give the radical cation  $[\mathbf{6}]^+$  is followed by a cyclodimerization process analogous to  
31  
32 that observed for oxidation of  $[\{\text{Ru}(\text{dppe})\text{Cp}\}_2(\mu\text{-C}\equiv\text{CC}\equiv\text{CC}\equiv\text{C})]^+$ .  
33  
34  
35  
36  
37  
38

39 While the radical cation  $[\mathbf{6}]^+$  is observed in the UV-vis-NIR spectra on oxidation, the  
40  
41 IR bands corresponding to  $[\mathbf{6}]^+$  were not observed in the IR spectra on oxidation. The  
42  
43 sample concentration used for IR spectroelectrochemistry is higher than for UV-vis-  
44  
45 NIR spectroelectrochemistry so the rate of dimerization on oxidation would likely be  
46  
47 faster and may account for the failure to detect any appreciable accumulation of  $[\mathbf{6}]^+$   
48  
49 in the IR experiments. Given the ample evidence for the highly reactive nature of  $[\mathbf{6}]^+$ ,  
50  
51 efforts to isolate this species were not undertaken.  
52  
53  
54  
55  
56  
57  
58  
59  
60

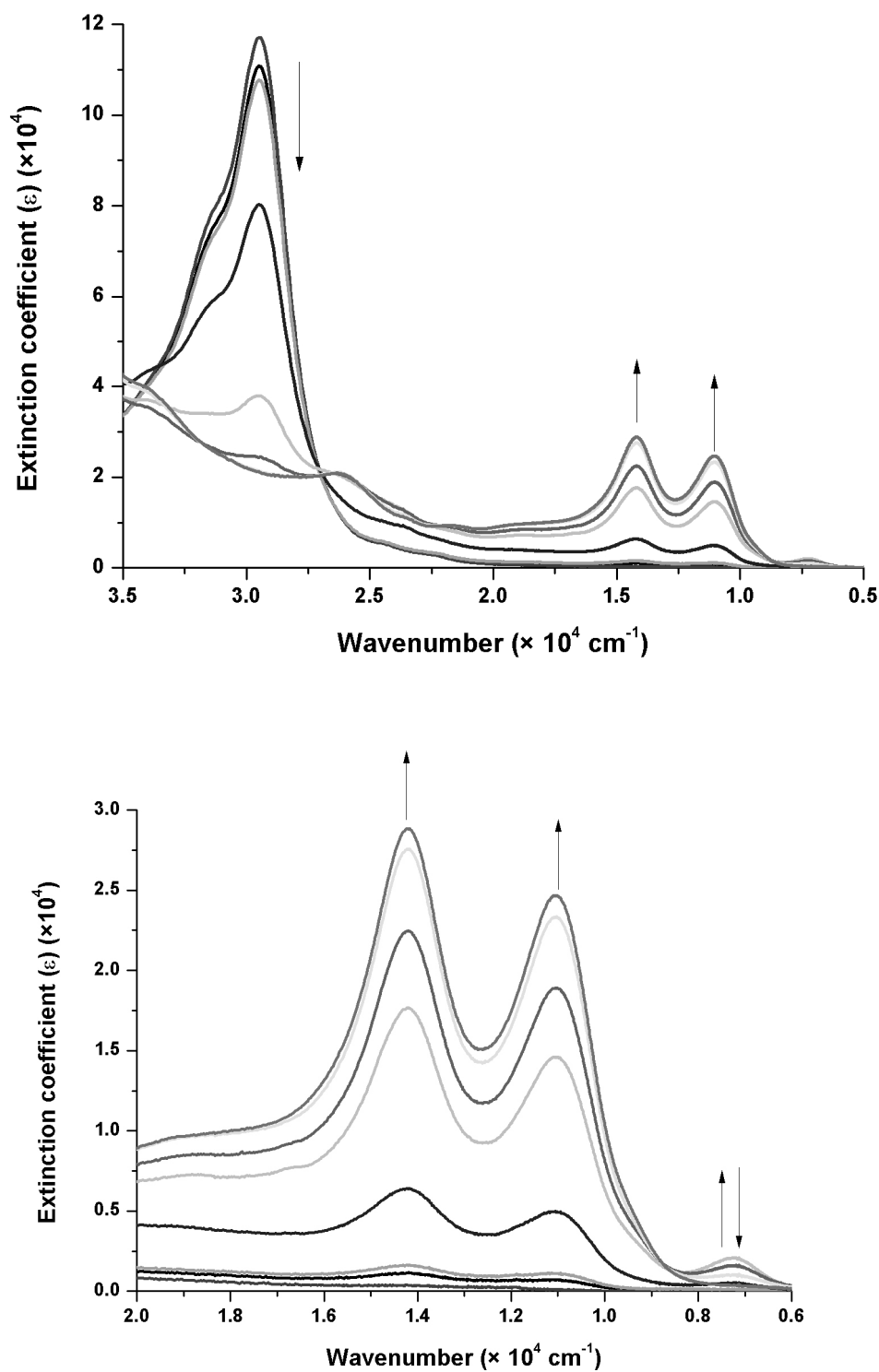


Fig 5. The UV-Vis-NIR spectra collected in a spectroelectrochemical cell during oxidation of **6** (0.1 M NBu<sub>4</sub>PF<sub>6</sub> / CH<sub>2</sub>Cl<sub>2</sub>).

### Quantum chemical calculations

The electronic structure of monometallic polyynyl<sup>8,89,90</sup> and bimetallic polyynediyl<sup>37-39, 87,91</sup> complexes has been explored in detail over the last 20 years at increasingly sophisticated levels of theory. Here, hybrid-DFT calculations (B3LYP/3-21G\*/CPCM-CH<sub>2</sub>Cl<sub>2</sub>) were carried out on the compounds **5** and **6** to investigate the influence of the interpolated phenylene ring on the electronic structure of these  $\pi$ -extended, carbon-rich complexes. The compound **4a** was also studied to aid the assignment of <sup>13</sup>C NMR spectra in the series **4a – e**. Each system was fully optimized without symmetry constraints, with frequency calculations indicating each structure to be a true minimum. The resulting computational systems are denoted **4a'**, **5'** and **6'** to distinguish them from the physical complexes.

Each structure in the bimetallic complexes adopts mutual *trans*-arrangement of the Cp rings and, in the case of **5'**, the phenylene ring essentially bisects the P-Ru-P angles at each metal (Cp(0)-Ru(1)-C(5)-C(7): -172.9° (**5**); 165.26° (**5'**); Cp(0) is the centroid of the Cp ring). The selected bond lengths and angles for **4a'**, **5'** and **6'** summarized in Table 1 enable comparison with the crystallographically determined structures. The majority of experimental bond lengths are reproduced well with differences of < 0.02 Å. The most significant deviations arise from the Ru-P distances in **6**, which are overestimated by 0.04 - 0.06 Å, and the ±0.06 Å difference between the calculated C(3)-C(4) and C(4)-C(5) distances in **5'** and the values obtained from the relatively low precision crystallographic structure. Nevertheless, deviations of this magnitude are



not uncommon for calculations of organometallic complexes and the overall level of agreement is more than satisfactory.

The electronic structures of **5'** (Table 3) and **6'** (Table 4) were also examined, those of buta-1,3-diynyl complexes having been well discussed elsewhere,<sup>8,89,90</sup> and give features that are broadly as expected for half-sandwich alkynyl-derivatives.<sup>92-94</sup> Thus, in each case the HOMO and HOMO-1 have  $d\pi/\pi$  character along the Ru-C $\equiv$ C-...-C $\equiv$ C-Ru backbone, with the usual nodal planes between the formally singly-bonded atoms (Figure 6).

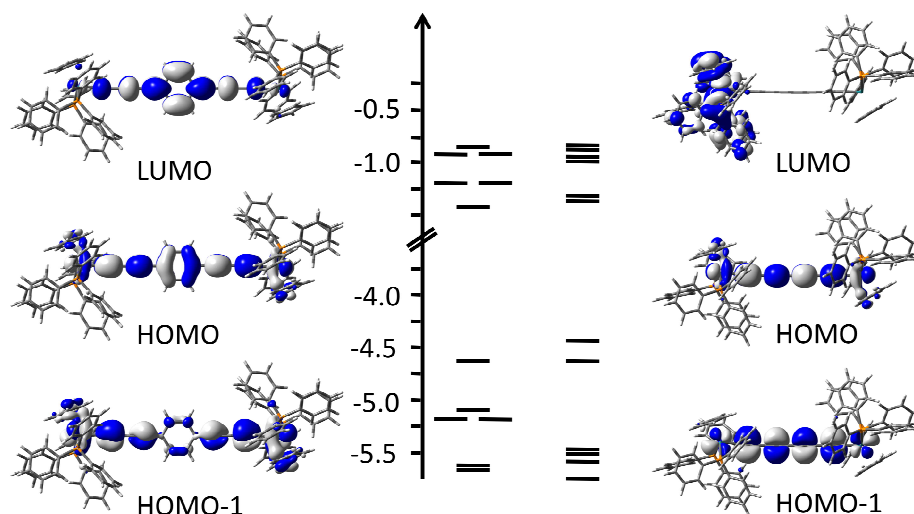


Figure 6. MO diagrams of **5'** (left) and **6'** (right) and plots of key frontier molecular orbitals (contour value  $\pm 0.02$  (e/bohr<sup>3</sup>)<sup>1/2</sup>).

These filled frontier orbitals are well separated from the LUMO and LUMO+1 ( $\Delta E_{\text{HOMO-LUMO}}$ : 3.31 eV (**5'**), 3.20 eV (**6'**)), which in **6'** are essentially degenerate, and largely located on the  $\text{Ru}(\text{PPh}_3)_2\text{Cp}$  fragments. However, at this level of theory, in **5'** the LUMO is bis(butadiynyl)benzene  $\pi^*$  orbital in character, with the degenerate  $\text{Ru}(\text{PPh}_3)_2\text{Cp}$  metal-ligand anti-bonding orbitals forming the LUMO+1 and LUMO+2 and lying ca. 0.1 eV above the LUMO.

Whilst the  $d\pi/\pi$ -type HOMO of **5'** is delocalized extensively along the entire length of the  $\text{RuC}\equiv\text{CC}\equiv\text{CC}_6\text{H}_4\text{C}\equiv\text{CC}\equiv\text{CRu}$  chain (ca. 24% Ru, 48%  $\text{C}_4$ , 15%  $\text{C}_6\text{H}_4$ ), the planar phenylene moiety breaks the conjugation in the orthogonal HOMO–1 (ca. 38% Ru, 40%  $\text{C}_4$ , 4%  $\text{C}_6\text{H}_4$ ), and gives a substantial HOMO to HOMO–1 gap of ca. 0.5 eV. In contrast, the cylindrical symmetry of the all-carbon chain in **6'** results in a more similar composition and energy of the HOMO (–4.46 eV; 27% Ru, 62%  $\text{C}_8$ ) and HOMO–1 (–4.64 eV; 27% Ru, 67%  $\text{C}_8$ ). The presence of one (**5'**) or two (**6'**) occupied orbitals in the frontier region is consistent with the observation of two (**5'**) or four (**6'**) oxidation processes in these complexes. In addition, the lower lying HOMO of **5'** is consistent with the more positive redox potentials (Table 2) observed for the first and second processes of **5'** relative to **6'**.

Table 3. Orbital energies (eV) and composition (%) for selected frontier orbitals of **5'**.

| MO       | eV    | Cp1 | PPh <sub>3</sub> 1 | Ru1 | Cα1 | Cβ1 | Cγ1 | Cδ1 | C <sub>6</sub> H <sub>4</sub> | Cδ2 | Cχ2 | Cβ2 | Cα2 | Ru2 | PPh <sub>3</sub> 2 | Cp2 |
|----------|-------|-----|--------------------|-----|-----|-----|-----|-----|-------------------------------|-----|-----|-----|-----|-----|--------------------|-----|
| 405 L+5  | -0.81 | 4   | 76                 | 10  | 1   | 0   | 0   | 0   | 0                             | 0   | 0   | 0   | 0   | 1   | 8                  | 0   |
| 404 L+4  | -0.85 | 1   | 98                 | 1   | 0   | 0   | 0   | 0   | 0                             | 0   | 0   | 0   | 0   | 0   | 0                  | 0   |
| 403 L+3  | -0.85 | 0   | 0                  | 0   | 0   | 0   | 0   | 0   | 0                             | 0   | 0   | 0   | 0   | 1   | 98                 | 1   |
| 402 L+2  | -1.23 | 0   | 0                  | 0   | 0   | 0   | 0   | 0   | 0                             | 0   | 0   | 0   | 0   | 32  | 54                 | 14  |
| 401 L+1  | -1.23 | 14  | 54                 | 32  | 0   | 0   | 0   | 0   | 0                             | 0   | 0   | 0   | 0   | 0   | 0                  | 0   |
| 400 LUMO | -1.33 | 1   | 1                  | 2   | 8   | 0   | 11  | 3   | 49                            | 3   | 11  | 0   | 8   | 2   | 1                  | 1   |
| 399 HOMO | -4.64 | 3   | 3                  | 12  | 5   | 8   | 4   | 7   | 15                            | 7   | 4   | 8   | 5   | 12  | 3                  | 3   |
| 398 H-1  | -5.14 | 5   | 4                  | 20  | 3   | 10  | 1   | 7   | 4                             | 6   | 1   | 9   | 3   | 18  | 4                  | 5   |
| 397 H-2  | -5.2  | 1   | 1                  | 6   | 1   | 3   | 0   | 2   | 2                             | 11  | 2   | 15  | 6   | 40  | 5                  | 5   |
| 396 H-3  | -5.2  | 5   | 5                  | 40  | 6   | 15  | 2   | 11  | 2                             | 2   | 0   | 3   | 1   | 7   | 1                  | 1   |
| 395 H-4  | -5.61 | 19  | 16                 | 34  | 5   | 4   | 1   | 4   | 1                             | 1   | 0   | 1   | 1   | 6   | 3                  | 4   |
| 394 H-5  | -5.62 | 4   | 3                  | 6   | 1   | 1   | 0   | 1   | 1                             | 4   | 1   | 5   | 5   | 33  | 16                 | 19  |

Table 4. Orbital energies (eV) and composition (%) for selected frontier orbitals of **6'**.

| MO       | eV    | Cp1 | PPh <sub>3</sub> 1 | Ru1 | Cα1 | Cβ1 | Cχ1 | Cδ1 | Cδ2 | Cχ2 | Cβ2 | Cα2 | Ru2 | PPh <sub>3</sub> 2 | Cp2 |
|----------|-------|-----|--------------------|-----|-----|-----|-----|-----|-----|-----|-----|-----|-----|--------------------|-----|
| 385 L+5  | -0.81 | 2   | 31                 | 6   | 7   | 0   | 8   | 4   | 4   | 8   | 0   | 7   | 6   | 13                 | 3   |
| 384 L+4  | -0.82 | 2   | 60                 | 9   | 4   | 0   | 4   | 2   | 2   | 4   | 0   | 3   | 2   | 6                  | 1   |
| 383 L+3  | -0.88 | 1   | 68                 | 2   | 3   | 0   | 3   | 2   | 2   | 3   | 0   | 3   | 3   | 8                  | 1   |
| 382 L+2  | -0.9  | 0   | 3                  | 0   | 1   | 0   | 1   | 1   | 1   | 1   | 0   | 1   | 6   | 82                 | 2   |
| 381 L+1  | -1.25 | 0   | 0                  | 0   | 0   | 0   | 0   | 0   | 0   | 0   | 0   | 0   | 34  | 52                 | 15  |
| 380 LUMO | -1.26 | 15  | 53                 | 32  | 0   | 0   | 0   | 0   | 0   | 0   | 0   | 0   | 0   | 0                  | 0   |
| 379 HOMO | -4.46 | 3   | 3                  | 13  | 8   | 8   | 7   | 7   | 8   | 7   | 9   | 8   | 14  | 3                  | 3   |
| 378 H-1  | -4.64 | 1   | 1                  | 14  | 9   | 8   | 8   | 8   | 8   | 9   | 8   | 9   | 13  | 1                  | 1   |
| 377 H-2  | -5.44 | 7   | 6                  | 21  | 0   | 8   | 1   | 4   | 4   | 1   | 8   | 0   | 25  | 6                  | 8   |
| 376 H-3  | -5.46 | 13  | 10                 | 34  | 1   | 2   | 0   | 1   | 1   | 0   | 3   | 1   | 21  | 6                  | 7   |
| 375 H-4  | -5.56 | 10  | 7                  | 18  | 2   | 1   | 1   | 1   | 1   | 1   | 1   | 2   | 27  | 14                 | 17  |
| 374 H-5  | -5.88 | 4   | 7                  | 28  | 1   | 8   | 0   | 4   | 4   | 0   | 8   | 1   | 23  | 6                  | 4   |

## Conclusion

We have demonstrated that the availability of stable terminal buta-1,3-diynyl complexes makes Sonogashira cross-coupling protocols an appealing entry point for the preparation of a wide range of substituted buta-1,3-diynyl compounds, thereby avoiding the preparation of buta-1,3-diyne ligand precursors. The process is suitable for the preparation of ‘simple’ buta-1,3-diynyl complexes, i.e. those bearing substituents, which are chemically and functionally rather complex, such as 2,3-dihydrobenzo[*b*]thiophene (**4d**) and pyridine (**4e**), and more elaborate bis(diynyl) complexes such as **5**. Facile homo-coupling of  $\text{Ru}(\text{C}\equiv\text{CC}\equiv\text{CH})(\text{PPh}_3)_2\text{Cp}$  in the presence of Pd(II) / Cu(I) co-catalysts and air as an oxidant affords the octa-1,3,5,7-tetra-1,8-diyl complex **6**. Whilst the chemical reactivity of  $[\mathbf{5}]^+$  and  $[\mathbf{6}]^+$  prevented detailed analysis of these compounds by spectroelectrochemical methods, DFT calculations indicate the significant organic character in the frontier orbitals of **5'** and **6'**. The significant difference in the relative energy and composition of the HOMO-1 in these complexes is consistent with the trends in electrochemical properties. The work described here therefore extends the ‘chemistry on the complex’ approach to the preparation of complex organometallic compounds, and further illustrates the facile synthetic routes that may be developed using this strategy.

## Experimental

*General conditions.* All reactions were carried out in oven-dried glassware under oxygen-free argon atmosphere using standard Schlenk techniques. Diisopropylamine and triethylamine were purified by distillation from KOH, other reaction solvents were purified and dried using Innovative Technology SPS-400 and degassed before

1  
2  
3 use. The compounds  $\text{Ru}(\text{C}\equiv\text{CC}\equiv\text{CH})(\text{PPh}_3)_2\text{Cp}^{18}$  and **3d**<sup>95</sup> were prepared by literature  
4  
5 methods. Other reagents were purchased commercially and used as received. NMR  
6  
7 spectra were recorded in deuterated solvent solutions on Bruker Avance 400 MHz and  
8  
9 Varian VNMRs 700 MHz spectrometers and referenced against residual protio-  
10  
11 solvent resonances ( $\text{CHCl}_3$ :  $^1\text{H}$  7.26 ppm,  $^{13}\text{C}$  77.00 ppm and  $\text{CH}_2\text{Cl}_2$ :  $^1\text{H}$  5.32 ppm,  
12  
13  $^{13}\text{C}$  53.84 ppm). In the NMR peak assignments, the phenyl ring associated with the  
14  
15 dppe and  $\text{PPh}_3$  are denoted Ph, and Ar indicates any arylene group belonging to the  
16  
17 alkynyl ligands. NMR spectra for **4a-e**, **5** and **6** are depicted in Figures S1-S28. The  
18  
19  $\text{C}_\beta$ ,  $\text{C}_\gamma$  and  $\text{C}_\delta$   $^{13}\text{C}$  NMR peaks were assigned with the aid of computed GIAO-NMR  
20  
21 data and are listed in Table S1.  
22  
23  
24  
25  
26  
27  
28

29  
30 Matrix-assisted laser desorption ionization (MALDI) mass spectra were recorded  
31  
32 using an Autoflex II TOF/TOF mass spectrometer with a 337 nm laser. Infrared  
33  
34 spectra were recorded on a Thermo 6700 spectrometer from  $\text{CH}_2\text{Cl}_2$  solution in a cell  
35  
36 fitted with  $\text{CaF}_2$  windows. Electrochemical analyses were recorded using a BAS  
37  
38 CV50W electrochemical analyzer fitted with a three-electrode system consisting of a  
39  
40 Pt disk as working electrode, auxiliary and reference electrode from solution in  
41  
42  $\text{CH}_2\text{Cl}_2$  containing 0.1 M  $\text{NBu}_4\text{PF}_6$ . Plots of the CVs of **4a-e**, **5** and **6** are shown in  
43  
44 Figures S29-S32.  
45  
46  
47  
48  
49  
50

51 *X-ray crystallography.* Single-crystal X-ray data for compounds **4a,b,d** were  
52  
53 collected at 120(2) K on a Bruker SMART CCD 6000 (fine-focus sealed tube,  
54  
55 graphite-monochromator) and for compound **6** on a Bruker D8Venture (Photon 100  
56  
57 CMOS detector, I $\mu$ S microsource, focusing mirrors) diffractometers using Mo  $\text{K}\alpha$   
58  
59  
60

radiation ( $\lambda = 0.71073 \text{ \AA}$ ). The data for extremely small and weakly diffracting crystals of **5** were collected at 150(2) K on a Rigaku Saturn 724+ diffractometer at station I19 of the Diamond Light Source (UK) synchrotron (undulator,  $\lambda = 0.6889 \text{ \AA}$ ,  $\omega$ -scan,  $1.0^\circ/\text{frame}$ ). The temperature on the crystals was maintained with Cryostream (Oxford Cryosystems) open-flow nitrogen cooling devices. All structures were solved by direct methods and refined by full-matrix least squares on  $F^2$  for all data using SHELXL<sup>96</sup> and OLEX2<sup>97</sup> software. All non-disordered non-hydrogen atoms were refined with anisotropic displacement parameters; H atoms were placed in the calculated positions and refined in riding mode. One of the Cl atoms in the  $\text{CH}_2\text{Cl}_2$  solvate molecule in the structure **6** showed abnormal a.d.p.'s and was modelled as disordered over two positions with fixed SOF 0.8 and 0.2. The largest component was refined in anisotropic mode, the minor one was left isotropic. The attempts to model a possible disorder of corresponding carbon atom did not result in any improvement of the model and the atom was refined with full occupancy. Crystallographic data for the structures have been deposited with the Cambridge Crystallographic Data Centre as supplementary publications CCDC-1033080-1033084.

*General procedure for the preparation of the buta-1,3-diynyl ruthenium (II) complexes **4a**, **4b**, **4c**, **4d**, **4e**:* In a Schlenk flask, a mixture of  $\text{Ru}(\text{C}\equiv\text{CC}\equiv\text{CH})(\text{PPh}_3)_2\text{Cp}$  (**2**), 1.5 equivalents of the appropriate iodoaryl, 5%-mol  $\text{Pd}(\text{PPh}_3)_4$  and 10%-mol  $\text{CuI}$  was added to degassed diisopropylamine ( $\text{NHPr}^i_2$ ) (1 mL/mmol). The reaction mixture was heated at  $90^\circ\text{C}$  for 2 h after which time the heating bath was removed and the solution allowed to cool to room temperature. The resulting precipitate was collected by filtration, washed with cold hexane, dried, and washed with cold MeOH, and dried in air to give the final compound.

$Ru(C\equiv CC\equiv C-C_6H_4CN-4)(PPh_3)_2Cp$  (**4a**).<sup>98</sup> From **2** (100 mg, 0.135 mmol) and isolated as a honey-yellow colored solid. Yield: 53 mg, 0.063 mmol (47%). Single crystals suitable for X-ray diffraction were grown by slow diffusion of methanol into a  $CH_2Cl_2$  solution containing 5%  $NEt_3$ .  $^1H$  NMR (400 MHz,  $CDCl_3$ ):  $\delta$  7.43 (ABq, J = 8.2 Hz, 4H, Ar), 7.37-7.35 (m, 12H, Ph), 7.21-7.19 (m, 6H, Ph), 7.12-7.10 (m, 12H, Ph), 4.33 (s, 5H, Cp) ppm.  $^{31}P$  { $^1H$ } NMR (162 MHz,  $CDCl_3$ ):  $\delta$  48.2 (s) ppm.  $^{13}C$  { $^1H$ } NMR (700 MHz,  $CDCl_3$ ):  $\delta$  138.1-137.8 (m,  $Ph_i$ ), 134.1 (t, J = 24.7 Hz,  $C_\alpha$ ) 133.6 (t, J = 4.9 Hz,  $Ph_o$ ), 132.6 ( $HC_{Ar}$ ), 131.6 ( $C_{Ar}$ ), 131.5 ( $HC_{Ar}$ ), 128.7 ( $Ph_p$ ), 127.4 (t, J = 4.6 Hz,  $Ph_m$ ), 119.3 ( $C\equiv N$ ), 108.2 ( $C_{Ar}$ ), 96.0 ( $C_\beta$ ), 85.9 (Cp), 85.7 ( $C_\gamma$ ), 61.8 ( $C_\delta$ ) ppm. IR ( $CH_2Cl_2$ ):  $\nu(C\equiv CC\equiv C)$  2147 s, 2017 m  $cm^{-1}$ . MS (MALDI-TOF):  $m/z$  579.2 [ $M-PPh_3$ ]<sup>+</sup>, 719 [ $Ru(CO)(PPh_3)_2Cp$ ]<sup>+</sup>, 841 [ $M$ ]<sup>+</sup>. HR-ESI<sup>+</sup>-MS:  $m/z$  calcd for  $C_{52}H_{40}NP_2^{96}Ru$  836.1712; found 836.1737. Crystal data for **4a**:  $C_{52}H_{39}NP_2Ru$ , M = 840.85, monoclinic, space group  $P2_1/c$ , a = 14.2477(6), b = 16.6875(8), c = 17.3130(8) Å,  $\beta$  = 90.515(1)°, U = 4116.1(3) Å<sup>3</sup>, F(000) = 1728, Z = 4, Dc = 1.357 mg m<sup>-3</sup>,  $\mu$  = 0.496 mm<sup>-1</sup>. 64895 reflections were collected yielding 10431 unique data (R<sub>merge</sub> = 0.0691). Final  $wR_2(F^2)$  = 0.0818 for all data (505 refined parameters), conventional R<sub>1</sub>(F) = 0.0330 for 7972 reflections with  $I \geq 2\sigma$ , GOF = 1.007.

$Ru(C\equiv CC\equiv C-C_6H_4CH_3-4)(PPh_3)_2Cp$  (**4b**). From **2** (40 mg, 0.054 mmol) to give a yellow solid. Yield: 39 mg, 0.047 mmol (87%). Single crystals suitable for X-ray diffraction were grown by slow diffusion of methanol into a  $CH_2Cl_2$  solution containing 5%  $NEt_3$ .  $^1H$  NMR (400 MHz,  $CDCl_3$ ):  $\delta$  7.44-7.39 (m, 12H, Ph), 7.34-7.32 (m, 2H, Ar), 7.26-7.20 (m, 6H, Ph), 7.15-7.11(m, 12H, Ph), 7.05-7.03 (m, 2H,

Ar), 4.33 (s, 5H, Cp), 2.32 (s, 3H, CH<sub>3</sub>) ppm. <sup>31</sup>P{<sup>1</sup>H} NMR (162 MHz, CDCl<sub>3</sub>): δ 48.4 (s) ppm. <sup>13</sup>C{<sup>1</sup>H} NMR (700 MHz, CDCl<sub>3</sub>): δ 138.3-137.8 (m) (Ph<sub>i</sub>), 135.5 (C<sub>Ar</sub>), 133.6 (t, J = 5.1 Hz, Ph<sub>o</sub>), 132.0 (HC<sub>Ar</sub>), 128.4, 128.3 (HC<sub>Ar</sub> or Ph<sub>p</sub>), 127.1 (t, J = 4.6 Hz, Ph<sub>m</sub>), 122.8 (t, J = 24.9 Hz, C<sub>α</sub>), 122.7 (C<sub>Ar</sub>), 95.4 (C<sub>β</sub>), 85.4 (Cp), 79.3 (C<sub>γ</sub>), 62.7 (C<sub>δ</sub>), 21.1 (CH<sub>3</sub>) ppm. IR (CH<sub>2</sub>Cl<sub>2</sub>): ν(C≡CC≡C) 2159 s, 2021 m cm<sup>-1</sup>. MS (MALDI-TOF): *m/z* 568.2 [M-PPh<sub>3</sub>]<sup>+</sup>, 830.0 [M]<sup>+</sup>. HR-ESI<sup>+</sup>-MS: *m/z* calcd for C<sub>52</sub>H<sub>42</sub>P<sub>2</sub><sup>96</sup>Ru 824.1838; found 824.1862. *Crystal data for 4b*: C<sub>52</sub>H<sub>42</sub>P<sub>2</sub>Ru, M = 829.87, monoclinic, space group P2<sub>1</sub>/n, a = 12.9342(9), b = 23.3662(17), c = 13.3100(10) Å, β = 98.512(2)°, U = 3978.3(5) Å<sup>3</sup>, F(000) = 1712, Z = 4, D<sub>c</sub> = 1.386 mg m<sup>-3</sup>, μ = 0.511 mm<sup>-1</sup>. 45590 reflections were collected yielding 9605 unique data (R<sub>merg</sub> = 0.0997). Final wR<sub>2</sub>(F<sup>2</sup>) = 0.0860 for all data (497 refined parameters), conventional R<sub>1</sub>(F) = 0.0413 for 5906 reflections with I ≥ 2σ, GOF = 0.961.

*Ru(C≡CC≡C-C<sub>6</sub>H<sub>4</sub>OMe-4)(PPh<sub>3</sub>)<sub>2</sub>Cp (4c)*. From **2** (40 mg, 0.054 mmol) to give a yellow solid. Yield: 27 mg, 0.032 mmol (59%). <sup>1</sup>H NMR (400 MHz, CDCl<sub>3</sub>): δ 7.43-7.40 (m, 12H, Ph), 7.37 (d, J = 8.6 Hz, 2H, Ar), 7.24-7.20 (m, 6H, Ph), 7.15-7.11 (m, 12H, Ph), 6.79 (d, J = 8.6 Hz, 2H, Ar), 4.33 (s, 5H, Cp), 3.80 (s, 3H, OMe) ppm. <sup>31</sup>P{<sup>1</sup>H} NMR (162 MHz, CDCl<sub>3</sub>): δ 49.1(s) ppm. <sup>13</sup>C{<sup>1</sup>H} NMR (600 MHz, CDCl<sub>3</sub>): δ 158.0 (C<sub>Ar</sub>-OMe), 138.6-137.9 (m, Ph<sub>i</sub>), 133.7 (t, J = 5.1 Hz, Ph<sub>o</sub>), 133.5 (HC<sub>Ar</sub>), 128.5 (Ph<sub>p</sub>), 127.3 (t, J = 4.7 Hz, Ph<sub>m</sub>), 122.1 (t, J = 25.0 Hz, C<sub>α</sub>), 118.1 (C<sub>Ar</sub>), 113.6 (HC<sub>Ar</sub>), 95.4 (C<sub>β</sub>), 85.6 (Cp), 78.7 (C<sub>γ</sub>), 62.4 (C<sub>δ</sub>), 55.1 (O-CH<sub>3</sub>). IR (CH<sub>2</sub>Cl<sub>2</sub>): ν(C≡CC≡C) 2160, 2021 cm<sup>-1</sup>. MS (MALDI-TOF): *m/z* 584.1 [M-PPh<sub>3</sub>]<sup>+</sup>, 846.1 [M]<sup>+</sup>. HR-ESI<sup>+</sup>-MS: *m/z* calcd for C<sub>52</sub>H<sub>42</sub>OP<sub>2</sub><sup>96</sup>Ru 840.1787; found 840.1828.



*Ru(C≡C-C≡C-DHBT)(PPh<sub>3</sub>)<sub>2</sub>Cp* (**4d**). From **2** (40 mg, 0.054 mmol) to give a mustard-colored solid. Yield: 25 mg, 0.029 mmol (54%). Single crystals suitable for X-ray diffraction were grown by slow diffusion of methanol into a CH<sub>2</sub>Cl<sub>2</sub> solution containing 5% NEt<sub>3</sub>. <sup>1</sup>H NMR (400 MHz, CDCl<sub>3</sub>): δ 7.42-7.37 (m, 12H, Ph), 7.24-7.18 (m, 8H, Ph + Ar), 7.13-7.09 (m, 12H, Ph), 7.06 (d, J = 8.0 Hz, 1H, Ar), 4.32 (s, 5H, Cp), 3.35-3.31 (m, 2H), 3.24-3.20 (m, 2H) ppm. <sup>31</sup>P {<sup>1</sup>H} NMR (162 MHz, CDCl<sub>3</sub>): δ 48.4 (s) ppm. <sup>13</sup>C {<sup>1</sup>H} NMR (700 MHz, CDCl<sub>3</sub>): δ 139.8 (C<sub>Ar</sub>), 139.3 (C<sub>Ar</sub>), 138.3-138.1 (m, Ph<sub>i</sub>), 133.7 (t, J = 4.9 Hz, Ph<sub>o</sub>), 131.5 (HC<sub>Ar</sub>), 128.5 (Ph), 128.0 (HC<sub>Ar</sub>), 127.3 (t, J = 4.6 Hz, Ph<sub>m</sub>), 121.6 (C<sub>Ar</sub>), 121.5 (HC<sub>Ar</sub>), 95.5 (C<sub>β</sub>), 85.6 (Cp), 79.7 (C<sub>γ</sub>), 62.7 (C<sub>δ</sub>), 35.9 (CH<sub>2</sub>), 33.4 (CH<sub>2</sub>) ppm, the C<sub>α</sub> peak was not visible. IR (CH<sub>2</sub>Cl<sub>2</sub>): ν(C≡CC≡C) 2156, 2015 cm<sup>-1</sup>. MS (MALDI-TOF): *m/z* 719.1 [Ru(CO)(PPh<sub>3</sub>)<sub>2</sub>Cp]<sup>+</sup>, 875.2 [M]<sup>+</sup>. HR-ESI<sup>+</sup>-MS: *m/z* calcd for C<sub>53</sub>H<sub>42</sub>P<sub>2</sub>S<sup>96</sup>Ru 868.1558; found 868.1597. *Crystal data for 4d*: C<sub>53</sub>H<sub>42</sub>P<sub>2</sub>RuS, M = 873.94, monoclinic, space group P 2<sub>1</sub>/n, a = 11.2014(7), b = 16.3616(11), c = 22.0949(14) Å, β = 90.675(2)°, U = 4049.1(5) Å<sup>3</sup>, F(000) = 1800, Z = 4, D<sub>c</sub> = 1.434 mg m<sup>-3</sup>, μ = 0.556 mm<sup>-1</sup>. 66387 reflections were collected yielding 10767 unique data (R<sub>merg</sub> = 0.0420). Final wR<sub>2</sub>(F<sup>2</sup>) = 0.0423 for all data (682 refined parameters), conventional R<sub>1</sub>(F) = 0.0315 for 8977 reflections with I ≥ 2σ, GOF = 1.065.

*Ru(C≡CC≡C-C<sub>5</sub>H<sub>4</sub>N)(PPh<sub>3</sub>)<sub>2</sub>Cp* (**4e**). From **2** (50 mg, 0.067 mmol) to give a yellow powder. Yield: 33 mg, 0.040 mmol (60%). <sup>1</sup>H NMR (400 MHz, CD<sub>2</sub>Cl<sub>2</sub>): δ 8.40 (d, J = 6.1 Hz, 2H, Ar), 7.39-7.36 (m, 12H, Ph), 7.29-7.27 (m, 6H, Ph), 7.22 (d, J = 6.1 Hz,

2H, Ar), 7.18-7.15 (m, 12H, Ph), 4.38 (s, 5H, Cp) ppm.  $^{31}\text{P}\{^1\text{H}\}$  NMR (162 MHz,  $\text{CDCl}_3$ ):  $\delta$  48.9 (s) ppm.  $^{13}\text{C}\{^1\text{H}\}$  NMR (600 MHz,  $\text{CDCl}_3$ ):  $\delta$  149.0 ( $\text{HC}_{\text{Ar}}$ ), 138.1-137.8 (m,  $\text{Ph}_i$ ), 134.6 ( $\text{C}_{\text{Ar}}$ ), 133.6 (t,  $J = 5.0$  Hz,  $\text{Ph}_o$ ), 128.7 ( $\text{Ph}_p$ ), 127.4 (t,  $J = 5.0$  Hz,  $\text{Ph}_m$ ), 126.4 ( $\text{HC}_{\text{Ar}}$ ), 95.7 ( $\text{C}_\beta$ ), 85.9 (Cp), 85.7 ( $\text{C}_\gamma$ ), 60.4 ( $\text{C}_\delta$ ), the  $\text{C}_\alpha$  peak was not visible. IR ( $\text{CH}_2\text{Cl}_2$ ):  $\nu(\text{C}\equiv\text{CC}\equiv\text{C})$  2150 m, 2006  $\text{cm}^{-1}$ . MS (MALDI-TOF):  $m/z$  817.1,  $[\text{M}]^+$ . HR-ESI $^+$ -MS:  $m/z$  calcd for  $\text{C}_{50}\text{H}_{40}\text{NP}_2^{96}\text{Ru}$  812.1712; found 812.1740.

$\{Ru(\text{PPh}_3)_2\text{Cp}\}_2(\mu\text{-C}\equiv\text{C-C}\equiv\text{CC}_6\text{H}_5\text{C}\equiv\text{C-C}\equiv\text{C})$  (5). A solution of  $\text{Ru}(\text{C}\equiv\text{CC}\equiv\text{CH})(\text{PPh}_3)_2\text{Cp}$  (2) (100 mg, 0.135 mmol), 1,4-diiodobenzene (23 mg, 0.067 mmol),  $\text{Pd}(\text{PPh}_3)_4$  (7 mg, 0.006 mmol) and  $\text{CuI}$  (2 mg, 0.012 mmol) in diisopropylamine (10 mL) was stirred for 2 h at room temperature before being heated at reflux for 2 h. The solvent was removed, and the residue purified on a neutral alumina column eluted with  $\text{CH}_2\text{Cl}_2:\text{NEt}_3$  (95:5 v/v). The yellow band was collected and reduced to the minimum volume prior to addition of MeOH (5 mL). On further concentration, a gold-brown solid precipitated which was collected by filtration, washed with MeOH and air-dried. Yield: 70 mg, 0.045 mmol (67%). Single crystals suitable for X-ray diffraction were grown by slow diffusion of diethyl ether into a  $\text{CH}_2\text{Cl}_2$  solution containing 5%  $\text{NEt}_3$ .  $^1\text{H}$  NMR (400 MHz,  $\text{CDCl}_3$ ):  $\delta$  7.44-7.29 (m, 24H, Ph), 7.30 (s, 4H, Ar), 7.25-7.21 (m, 12H, Ph), 7.15-7.12 (m, 24H, Ph), 4.34 (s, 10H,  $\text{H}_{\text{Cp}}$ ) ppm.  $^{31}\text{P}\{^1\text{H}\}$  NMR (162 MHz,  $\text{CDCl}_3$ ):  $\delta$  48.4 (s) ppm.  $^{13}\text{C}\{^1\text{H}\}$  NMR (700 MHz,  $\text{CDCl}_3$ ):  $\delta$  138.3-138.1 ( $\text{Ph}_i$ ), 133.7 (t,  $J = 5.0$  Hz,  $\text{Ph}_o$ ), 131.8 ( $\text{HC}_{\text{Ar}}$ ), 128.5 ( $\text{Ph}_p$ ), 127.3 (t,  $J = 4.7$  Hz,  $\text{Ph}_m$ ), 125.7 (t,  $J = 23.0$  Hz,  $\text{C}_\alpha$ ), 123.4 ( $\text{C}_{\text{Ar}}$ ), 95.9 ( $\text{C}_\beta$ ), 85.6 (Cp), 81.8 ( $\text{C}_\gamma$ ), 63.4 ( $\text{C}_\delta$ ), the  $\text{C}_\alpha$  peak was not visible. IR ( $\text{CH}_2\text{Cl}_2$ ):  $\nu(\text{C}\equiv\text{CC}\equiv\text{C})$  2155 s, 2016 m  $\text{cm}^{-1}$ . MS (MALDI-TOF;  $m/z$ ): 1554.0  $[\text{M}]^+$ . HR-ESI $^+$ -

MS:  $m/z$  calcd for  $C_{96}H_{74}P_4Ru_2$  1554.2871; found: 1554.2665. *Crystal data for 5*:  $C_{96}H_{74}P_4Ru_2 \cdot CH_2Cl_2$ ,  $M = 1638.50$ , monoclinic, space group  $P2_1/c$ ,  $a = 16.693(7)$ ,  $b = 11.384(4)$ ,  $c = 21.646(9)$  Å,  $\beta = 98.678(5)^\circ$ ,  $U = 4066(3)$  Å<sup>3</sup>,  $F(000) = 1680$ ,  $Z = 2$ ,  $D_c = 1.338$  mg m<sup>-3</sup>,  $\mu = 0.563$  mm<sup>-1</sup>. 20671 reflections were collected yielding 6114 unique data ( $R_{\text{merge}} = 0.0929$ ). Final  $wR_2(F^2) = 0.2575$  for all data (487 refined parameters), conventional  $R_1(F) = 0.0800$  for 3957 reflections with  $I \geq 2\sigma$ , GOF = 1.024. Due to extremely weak diffraction only reflections with  $2\theta \leq 46^\circ$  were used in the refinement.

$\{Ru(PPh_3)_2Cp\}_2(\mu-C \equiv CC \equiv CC \equiv CC \equiv C)$  (**6**). An open flask was charged with a solution of  $Ru(C \equiv CC \equiv CH)(PPh_3)_2Cp$  (**2**) (100 mg, 0.135 mmol),  $Pd(PPh_3)_4$  (6.8 mg, 0.006 mmol) and an excess of  $CuI$  (8 mg) in  $NHPr^i_2$  (8 mL). The mixture was stirred at room temperature for 1 h after which time the solution had turned yellow and a brown precipitate had formed. The solvent was removed and the residue purified on a neutral alumina column eluted by  $CH_2Cl_2/5\%$   $NEt_3$ . After precipitation from hexane a bright yellow solid was obtained. Yield: 55 mg, 0.037 mmol (55%). Crystals suitable for X-ray diffraction were obtained from  $CH_2Cl_2 / Et_2O$  by slow diffusion.  $^1H$  NMR (400 MHz,  $CD_2Cl_2$ ):  $\delta$  7.42-7.38 (m, 24H, Ph), 7.24-7.21 (m, 12H, Ph), 7.15-7.11 (m, 24H, Ph), 4.31 (s, 10H, Cp) ppm.  $^{31}P\{^1H\}$  NMR (162 MHz,  $CDCl_3$ ):  $\delta$  48.9 (s) ppm.  $^{13}C\{^1H\}$  NMR (600 MHz,  $CD_2Cl_2$ ):  $\delta$  138.9-138.3 ( $Ph_i$ ), 134.1 (t,  $J = 5.0$  Hz,  $Ph_o$ ), 129.2 ( $Ph_p$ ), 127.8 (t,  $J = 4.6$  Hz,  $Ph_m$ ), 119.6 (t,  $J = 24.9$  Hz,  $C_\alpha$ ), 96.7 ( $C_\beta$ ), 86.4 (Cp), 62.6 ( $C_\gamma$ ), 51.7 ( $C_\delta$ ). IR ( $CH_2Cl_2$ ):  $\nu((C \equiv C)_4)$  2107 s, 1955 m cm<sup>-1</sup>. MS<sup>+</sup> (MALDI-TOF):  $m/z$  954.1  $[M-2PPh_3]^+$ , 1216.1  $[M-PPh_3]^+$ , 1478  $[M]^+$ . HR-ESI<sup>+</sup>-MS:  $m/z$  calcd for  $C_{90}H_{70}P_4Ru_2$  1478.2556; found 1478.2368. Calculated for

C<sub>91</sub>H<sub>70</sub>P<sub>4</sub>Ru<sub>2</sub>·0.5CH<sub>2</sub>Cl<sub>2</sub>: C, 71.51; H, 4.71. Found: C, 71.85; H, 4.80. *Crystal data for 6*: C<sub>90</sub>H<sub>70</sub>P<sub>4</sub>Ru<sub>2</sub>·2CH<sub>2</sub>Cl<sub>2</sub>, M = 1647.33, triclinic, space group P -1, a = 8.8692(4), b = 12.6858(5), c = 17.6885(7) Å, α = 90.25(2), β = 96.49(2), γ = 96.49(2)°, U = 1895.35(14) Å<sup>3</sup>, F(000) = 842, Z = 1, D<sub>c</sub> = 1.443 mg m<sup>-3</sup>, μ = 0.672 mm<sup>-1</sup>. 32488 reflections were collected yielding 8724 unique data (R<sub>merg</sub> = 0.1696). Final wR<sub>2</sub>(F<sup>2</sup>) = 0.1745 for all data (464 refined parameters), conventional R<sub>1</sub>(F) = 0.0753 for 5362 reflections with I ≥ 2σ, GOF = 0.991.

## Computations

All hybrid-DFT computations were carried out with the Gaussian 09 package.<sup>99</sup> The geometries of **4a**, **5** and **6** discussed here were optimized at the B3LYP/3-21G\* level of theory<sup>100,101</sup> with no symmetry constraints with the polarized solvent continuum model (dichloromethane) applied.<sup>102</sup> These geometries revealed no imaginary frequencies indicating true minima. Electronic structure calculations were also carried out at the B3LYP/3-21G\* level of theory. The MO diagrams and orbital contributions were generated with the aid of GaussView 5.0 and GaussSum packages respectively.<sup>103,104</sup> Theoretical <sup>13</sup>C NMR chemical shifts obtained at the GIAO<sup>105</sup>-B3LYP/3-21G\*//B3LYP/3-21G\* level on the optimized geometries were referenced to TMS: δ(<sup>13</sup>C) = 207.1 – σ(<sup>13</sup>C).

**Acknowledgements** The authors thank EPSRC and ARC for funding and are grateful to the Diamond Light Source for an award of instrument time on the Station I19 (MT 6749) and the instrument scientists for support. PJJ held an EPSRC Leadership Fellowship and holds an ARC Future Fellowship (FT120100073).

**Supporting Information.** Plots of  $^1\text{H}$ ,  $^{13}\text{C}$  and  $^{31}\text{P}$  NMR spectra. Plots of cyclic voltammograms for **4a-4e**, **5** and **6** and of  $i_{\text{pa}}$  vs  $\sqrt{v}$  for **4a-4e**. Plots of molecules of **4b** and **4d**. Table comparing observed and computed (GIAO/NMR)  $^{13}\text{C}$  NMR shifts for  $C_\beta$ ,  $C_\gamma$  and  $C_\delta$  carbons in **4a**, **5** and **6**. CIF files for compounds **4a**, **4b**, **4d**, **5** and **6**. A text file of Cartesian coordinates for **4a'**, **5'** and **6'** in a format for convenient visualization. This material is available free of charge via the Internet at <http://pubs.acs.org>.

### Dedication.

Dedicated to the memory of Professor Michael F. Lappert, one of the true pioneers in synthetic organometallic chemistry and an example to us all.

### References

1. Akita, M.; Chung, M.-C.; Sakurai, A.; Sugimoto, S.; Terada, M.; Tanaka, M.; Moro-oka, Y. *Organometallics* **1997**, *16*, 4882-4691.
2. Mohr, W.; Stahl, J.; Hampel, F.; Gladysz, J.A. *Chem. Eur. J.* **2003**, *9*, 3324-3340.
3. Owen, G.R.; Stahl, J.; Hampel, F.; Gladysz, J.A. *Organometallics* **2004**, *23*, 5889-5892.
4. Stahl, J.; Bohling, J.C.; Peters, T.B.; de Quadras, L.; Gladysz, J.A. *Pure Appl. Chem.* **2008**, *80*, 459-474.
5. Bruce, M.I.; Low, P.J.; Ke, M.; Kelly, B.D.; Skelton, B.W.; Smith, M.E.; White, A.H.; Witton, N.B. *Aust. J. Chem.* **2001**, *54*, 453-460.
6. Roberts, R.L.; Puschmann, H.; Howard, J.A.K.; Yamamoto, J.H.; Carty, A.J.; Low, P.J. *Dalton Trans.* **2003**, 1099-1105.
7. Bruce, M.I.; Costuas, K.; Davin, T.; Ellis, B.G.; Halet, J.-F.; Lapinte, C.; Low, P.J.; Smith, M.E.; Skelton, B.W.; Toupet, L.; White, A.H. *Organometallics* **2005**, *24*, 3864-3881.

8. Gendron, F.; Burgun, A.; Skelton, B.W.; White, A.H.; Roisnel, T.; Bruce, M.I.; Halet, J.-F.; Lapinte, C.; Costuas, K. *Organometallics* **2012**, *31*, 6796-6811.
9. Bruce, M.I.; Scoleri, N.; Skelton B.W. *J. Organomet. Chem.* **2011**, *696*, 3473-3482.
10. Bruce, M.I.; Jevric, M.; Skelton, B.W.; Smith, M.E.; White, A.H.; Zaitseva, N.N. *J. Organomet. Chem.* **2006**, *691*, 361-370.
11. Paul, F.; Meyer, W.E.; Toupet, L.; Jiao, H.; Gladysz, J.A.; Lapinte, C. *J. Am. Chem. Soc.* **2000**, *122*, 9405-9414.
12. Bartlett, M.J.; Hill, A.F.; Smith, M.K. *Organometallics* **2005**, *24*, 5795-5798.
13. Moreno, C.; Arnanz, A.; Delgado, S. *Inorg. Chim. Acta* **2001**, *312*, 139-150.
14. Bruce, M.I.; Ellis, B.G.; Skelton, B.W.; White, A.H. *J. Organomet. Chem.* **2000**, *607*, 137-145.
15. Bruce, M.I.; Costuas, K.; Halet, J.F.; Hall, B.C.; Low, P.J.; Nicholson, B.K.; Skelton, B.W.; White, A.H. *J. Chem. Soc., Dalton Trans.* **2002**, 383-398.
16. Bruce, M.I.; Hall, B.C.; Skelton, B.W.; Smith, M.E.; White, A.H. *J. Chem. Soc., Dalton Trans.* **2002**, 995-1001.
17. Bruce, M.I.; Halet, J.-F.; Le Guennic, B.; Skelton, B.W.; Smith, M.E.; White, A.H. *Inorg. Chim. Acta* **2003**, *350*, 175-181.
18. Bruce, M.I.; Ellis, B.G.; Gaudio, M.; Lapinte, C.; Melino, G.; Giovanni, P.; Paul, F.; Skelton, B.W.; Smith, M.E.; Toupet, L.; White, A.H. *Dalton Trans.* **2004**, 1601-1609.
19. Bruce, M.I.; Low, P.J.; Nicholson, B.K.; Skelton, B.W.; Zaitseva, N.N.; Zhao, X.-I. *J. Organomet. Chem.* **2010**, *695*, 1569-1575.
20. Bruce, M.I.; Büschel, S.; Cole, M.L.; Scoleri, N.; Skelton, B.W.; White, A.H.; Zaitseva, N.N. *Inorg. Chim. Acta* **2012**, *382*, 6-12.
21. Bruce, M.I.; Le Guennic, B.; Scoleri, N.; Zaitseva, N.N.; Halet, J.-F. *Organometallics* **2012**, *31*, 4701-4706.
22. Ying, J.-W.; Liu, I.-P.; Xi, B.; Song, Y.; Campana, C.; Zuo, J.-L.; Ren, T. *Angew. Chem. Int. Ed.* **2010**, *49*, 954-957.
23. Bear, J.L.; Han, B.; Wu, Z.; Van Caemelbecke, E.; Kadish, K.M. *Inorg. Chem.* **2001**, *40*, 2275-2281.
24. Falloon, S.B.; Arif, A.M.; Gladysz, J.A. *Chem. Commun.* **1997**, 629-630.

25. Semenov, S.N.; Taghipourian, S.F.; Blacque, O.; Fox, T.; Venkatesan, K.; Berke, H. *J. Am. Chem. Soc.* **2010**, *132*, 7584-7585.
26. Lissel, F.; Fox, T.; Blacque, O.; Polit, W.; Winter, R.F.; Venkatesan, K.; Berke, H. *J. Am. Chem. Soc.* **2013**, *135*, 4051-4060.
27. AlQaiai, S.M.; Galat, K.J.; Chai, M.H.; Ray, D.G.; Rinaldi, P.L.; Tessier, C.A.; Youngs, W.J. *J. Am. Chem. Soc.* **1998**, *120*, 12149-12150.
28. Horn, C.R.; Gladysz, J.A. *Eur. J. Inorg. Chem.* **2003**, 2211-2218.
29. Owen, G.R.; Hampel, F.; Gladysz, J.A. *Organometallics* **2004**, *23*, 5893-5895.
30. Chisholm, M.H. *Angew. Chem. Int. Ed. Engl.* **1991**, *30*, 673-674.
31. Takahashi, S.; Kariya, M.; Yatake, T.; Sonogashira, K.; Hagihara, N. *Macromol.* **1978**, *11*, 1063-1066.
32. Hagihara, N.; Sonogashira, K.; Takahashi, S. *Adv. Polym. Sci.* **1981**, *41*, 149-179.
33. Fyfe, H.B.; Mlekuz, M.; Zargarian, D.; Taylor, N.J.; Marder, T.B. *J. Chem. Soc., Chem. Commun.* **1991**, 188-190.
34. Marder, T.B.; Lesley, G.; Yuan, Z.; Fyfe, H.B.; Chow, P.; Stringer, G.; Jobe, I.R.; Taylor, N.J.; Williams, I.D.; Kurtz, S.K. *ACS Symp. Ser.* **1991**, *455*, 605-615.
35. Fyfe, H.B.; Mlekuz, M.G.; Taylor, N.J.; Marder, T.B. *NATO ASI Ser., Ser. E*, **2006**, 331-344.
36. Frapper, G.; Kertesz, M. *Inorg. Chem.* **1993**, *32*, 732-740.
37. Belanzoni, P.; Re, N.; Sgamellotti, A.; Floriani, C. *J. Chem. Soc., Dalton Trans.* **1998**, 1825-1835.
38. Zhuravlev, F.; Gladysz, J.A. *Chem. Eur. J.* **2004**, *10*, 6510-6522.
39. Costuas, K.; Rigaut, S. *Dalton Trans.* **2011**, *40*, 5643-5658.
40. Moreno, C.; Gómez, J.L.; Medina, R.-M.; Macazaga, M.-J.; Arnanz, A.; Lough, A.; Farrar, D.H.; Delgado, S. *J. Organomet. Chem.* **1999**, *579*, 63-74.
41. Weng, W.; Bartik, T.; Gladysz, J.A. *Angew. Chem. Int. Ed.* **1994**, *33*, 2199-2202.
42. Weng, W.; Bartik, T.; Brady, M.; Bartik, B.; Ramsden, J.A.; Arif, A.M.; Gladysz, J.A. *J. Am. Chem. Soc.* **1995**, *117*, 11922-11931.
43. Bartik, T.; Weng, W.; Ramsden, J.A.; Szafert, S.; Falloon, S.B.; Arif, A.M.; Gladysz, J.A. *J. Am. Chem. Soc.* **1998**, *120*, 11071-11081.

44. Bruce, M.I.; Scoleri, N.; Skelton, B.W.; White, A.H. *J. Organomet. Chem.* **2010**, *695*, 1561-1568.
45. Wong, A.; Kang, P.C.W.; Tagge, C.D.; Leon, D.R. *Organometallics* **1990**, *9*, 1992-1994.
46. de Quadras, L.; Shelton, A.H.; Kuhn, H.; Hampel, F.; Schanze, K.S.; Gladysz, J.A. *Organometallics* **2008**, *27*, 4979-4991.
47. Bruce, M.I.; Ke, M.; Low, P.J.; Skelton, B.W.; White, A.H. *Organometallics* **1998**, *17*, 3539-3549.
48. Denis, R.; Weyland, T.; Paul, F.; Lapinte, C. *J. Organomet. Chem.* **1997**, *545-546*, 615-618.
49. Le Stang, S.; Lenz, D.; Paul, F.; Lapinte, C. *J. Organomet. Chem.* **1999**, *572*, 189-192.
50. Denis, R.; Toupet, L.; Paul, F.; Lapinte, C. *Organometallics* **2000**, *19*, 4240-4251.
51. Courmarcel, J.; Le Gland, G.; Toupet, L.; Paul, F.; Lapinte, C. *J. Organomet. Chem.* **2003**, *670*, 108-122.
52. Hurst, S.K.; Cifuentes, M.P.; McDonagh, A.M.; Humphrey, M.G.; Samoc, M.; Luther-Davies, B.; Asselberghs, I.; Persoons, A. *J. Organomet. Chem.* **2002**, *642*, 259-267.
53. Brady, M.; Weng, W.Q.; Gladysz, J.A. *J. Chem. Soc., Chem. Commun.* **1994**, 2655-2656.
54. Bartik, T.; Bartik, B.; Brady, M.; Dembinski, R.; Gladysz, J.A. *Angew. Chem., Int. Ed.* **1996**, *35*, 414-417.
55. Bartik, B.; Dembinski, R.; Bartik, T.; Arif, A.M.; Gladysz, J.A. *New. J. Chem.* **1997**, *21*, 739-750.
56. Dembinski, R.; Lis, T.; Szafert, S.; Mayne, C.L.; Bartik, T.; Gladysz, J.A. *J. Organomet. Chem.* **1999**, *578*, 229-246.
57. Peters, T.B.; Bohling, J.C.; Arif, A.M.; Gladysz, J.A. *Organometallics* **1999**, *18*, 3261-3263.
58. Dembinski, R.; Bartik, T.; Bartik, B.; Jaeger, M.; Gladysz, J.A. *J. Am. Chem. Soc.* **2000**, *122*, 810-822.
59. Meyer, W.E.; Amoroso, A.J.; Horn, C.R.; Jaeger, M.; Gladysz, J.A. *Organometallics* **2001**, *20*, 1115-1127.



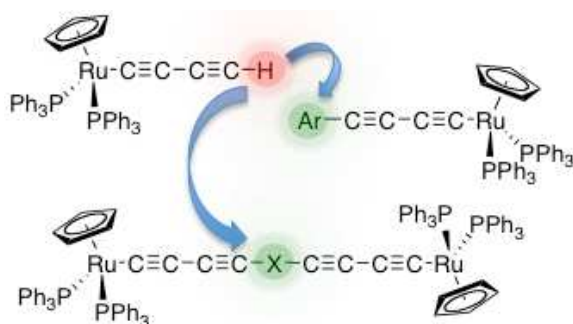
- 1  
2  
3 60. Mohr, W.; Stahl, J.; Hampel, F.; Gladysz, J.A. *Inorg. Chem.*, **2001**, *40*, 3263-  
4 3264.  
5  
6 61. Zheng, Q.; Gladysz, J.A. *J. Am. Chem. Soc.* **2005**, *127*, 10508-10509.  
7  
8 62. Zheng, Q.; Bohling, J.C.; Peters, T.B.; Frisch, A.C.; Hampel, F.; Gladysz, J.A.  
9 *Chem. Eur. J.* **2006**, *12*, 6486-6505.  
10  
11 63. Bruce, M.I.; Kramarczuk, K.A.; Zaitseva, N.N.; Skelton, B.W.; White, A.H. *J.*  
12 *Organomet. Chem.* **2005**, *690*, 1549-1555.  
13  
14 64. Antonova, A.B.; Bruce, M.I.; Ellis, B.G.; Gaudio, M.; Humphrey, P.A.; Jevric,  
15 M.; Melino, G.; Nicholson, B.K.; Perkins, G.J.; Skelton, B.W.; Stapleton, B.;  
16 White, A.H.; Zaitseva, N.N. *Chem. Commun.* **2004**, 960-961.  
17  
18 65. Ren, T. *Chem. Rev.* **2008**, *108*, 4185-4207.  
19  
20 66. Burgun, A.; Gendron, F.; Roisnel, T.; Sinbandhit, S.; Costuas, K.; Halet, J.-F.;  
21 Bruce, M.I.; Lapinte, C. *Organometallics* **2013**, *32*, 1866-1875.  
22  
23 67. Bruce, M.I.; Costuas, K.; Gendron, F.; Halet, J.-F.; Jevric, M.; Skelton, B.W.  
24 *Organometallics* **2012**, *31*, 6555-6566.  
25  
26 68. Burgun, A.; Gendron, F.; Schauer, P.A.; Skelton, B.W.; Low, P.J.; Costuas,  
27 K.; Halet, J.-F.; Bruce, M.I.; Lapinte, C. *Organometallics* **2013**, *32*, 5015-  
28 5025  
29  
30 69. Bruce, M.I.; Burgun, A.; Grelaud, G.; Jevric, M.; Nicholson, B.K.; Skelton,  
31 B.W.; White, A.H.; Zaitseva, N.N. *Z. Anorg. Allg. Chem.* **2011**, *637*, 1334-  
32 1340.  
33  
34 70. Low, P.J.; Bruce, M.I. *Adv. Organomet. Chem.* **2002**, *48*, 71-288.  
35  
36 71. Nguyen, P.; Zheng, Y.A.; Agocs, L.; Lesley, G.; Marder, T.B. *Inorg. Chim.*  
37 *Acta* **1994**, *220*, 289-296.  
38  
39 72. Batsanov, A.S.; Collings, J.C.; Fairlamb, I.J.S.; Holland, J.P.; Howard, J.A.K.;  
40 Lin, Z.Y.; Marder, T.B.; Parsons, A.C.; Ward, R.M.; Zhu, J. *J. Org. Chem.*  
41 **2005**, *70*, 703-706.  
42  
43 73. Liu, Q.; Burton, D.J. *Tetrahedron Lett.* **1997**, *38*, 4371-4374.  
44  
45 74. Rossi, R.; Carpita, A.; Bigelli, C. *Tetrahedron Lett.* **1985**, *26*, 523-526.  
46  
47 75. Hay, A.S. *J. Org. Chem.* **1962**, *27*, 3320-3321.  
48  
49 76. Bruce, M.I.; Kelly, B.D.; Skelton, B.W.; White, A.H. *J. Organomet. Chem.*  
50 **2000**, *604*, 150-156.  
51  
52 77. Bruce, M.I.; Hall, B.C.; Kelly, B.D.; Low, P.J.; Skelton, B.W.; White, A.H. *J.*  
53 *Chem. Soc., Dalton Trans.* **1999**, 3719-3728.  
54  
55  
56  
57  
58  
59  
60

- 1  
2  
3 78. Coat, F.; Lapinte, C. *Organometallics* **1996**, *15*, 477-479.  
4  
5 79. Zheng, Q.; Hampel, F.; Gladysz, J.A. *Organometallics* **2004**, *23*, 5896-5899.  
6  
7 80. de Quadras, L.; Hampel, F.; Gladysz, J.A. *Dalton Trans.* **2006**, 2929-2933.  
8  
9 81. Peters, T. B.; Zheng, Q.; Stahl, J.; Bohling, J.C.; Arif, A.M.; Hampel, F.;  
10 Gladysz, J.A. *J. Organomet. Chem.* **2002**, *641*, 53-61.  
11  
12 82. Bruce, M.I.; Cole, M.L.; Ellis, B.G.; Gaudio, M.; Nicholson, B.K.; Parker,  
13 C.R.; Skelton, B.W.; White, A.H. *Polyhedron* **2015**, *86*, 43-56.  
14  
15 83. Bock, S.; Eaves, S.G.; Parthey, M.; Kaupp, M.; Le Guennic, B.; Halet, J.-F.;  
16 Yufit, D.S.; Howard, J.A.K.; Low, P.J. *Dalton Trans.*, **2013**, *42*, 4240-4243.  
17  
18 84. Zafert, S.; Gladysz, J.A. *Chem. Rev.* **2006**, *106*, PR1-PR33  
19  
20 85. Schauer, P.A.; Low, P.J. *Eur. J. Inorg. Chem.* **2012**, *3*, 390-411.  
21  
22 86. Bruce, M.I.; Low, P.J.; Costuas, K.; Halet, J.-F.; Best, S.P.; Heath, G.A. *J.*  
23 *Am. Chem. Soc.* **2000**, *122*, 1949-1962.  
24  
25 87. Parthey, M.; Gluyas, J.B.G.; Schauer, P.A.; Yufit, D.S.; Howard, J.A.K.;  
26 Kaupp, M.; Low, P.J. *Chem. Eur. J.* **2013**, *19*, 9780-9784.  
27  
28 88. Krejcik, M.; Danek, M.; Hartl, F. *J. Electroanal. Chem.* **1991**, *317*, 179-187.  
29  
30 89. Lichtenberger, D.L.; Renshaw, S.K.; Wong, A.; Tagge, C.D. *Organometallics*  
31 **1993**, *12*, 3522-3536.  
32  
33 90. Koentjoro, O.F.; Rousseau, R.; Low, P.J. *Organometallics* **2001**, *20*, 4502-  
34 4509.  
35  
36 91. Herrmann, C.; Neugebauer, J.; Gladysz, J.A.; Reiher, M. *Inorg. Chem.* **2005**,  
37 *44*, 6174-6182.  
38  
39 92. Fox, M.A.; Roberts, R.L.; Khairul, W.M.; Hartl, F.; Low, P.J. *J. Organomet.*  
40 *Chem.* **2007**, *692*, 3277-3290.  
41  
42 93. McGrady, J.E.; Lovell, T.; Stranger, R.; Humphrey, M.G. *Organometallics*  
43 **1997**, *16*, 4004-4011.  
44  
45 94. Paul, F.; Ellis, B.G.; Bruce, M.I.; Toupet, L.; Roisnel, T.; Costuas, K.; Halet,  
46 J.F.; Lapinte, C. *Organometallics* **2006**, *25*, 649-665.  
47  
48 95. Moreno-García, P.; Gulcur, M.; Manrique, D. Z.; Pope, T.; Hong, W.;  
49 Kaliginedi, V.; Huang, C.; Batsanov, A.S.; Bryce, M.R.; Lambert, C.;  
50 Wandlowski, T. *J. Am. Chem. Soc.* **2013**, *135*, 12228-12240.  
51  
52 96. Sheldrick, G.M. *Acta Cryst., Sect. A.* **2008**, *64*, 112-122.  
53  
54 97. Dolomanov, O.V.; Bourhis, L.J.; Gildea, R.J.; Howard, J.A.K.; Puschmann, H.  
55 *J. Appl. Cryst.* **2009**, *43*, 339-341.  
56  
57  
58  
59  
60

- 1  
2  
3 98. Whilst compound **4b** analyzed well, and **6** as a partial CH<sub>2</sub>Cl<sub>2</sub> solvate  
4  
5 (consistent with the crystallographic work and the <sup>1</sup>H NMR spectrum) the  
6  
7 other complexes consistently analyzed very low in carbon. For example **4c**:  
8  
9 C<sub>52</sub>H<sub>42</sub>OP<sub>2</sub>Ru C, 73.83; H, 5.00. Found C, 71.45; H, 4.31. **4d**: C<sub>53</sub>H<sub>42</sub>P<sub>2</sub>RuS C,  
10  
11 72.84; H, 4.84. Found C, 68.75; H, 4.89. It is known that unsaturated,  
12  
13 acetylene-rich compounds can thermally polymerize to give some  
14  
15 extraordinarily robust thermoset carbonaceous materials; see, for example, (a)  
16  
17 Stephens, E.B.; Tour, J.M. *Adv. Mater.* **1992**, 4, 570-572 (b) Stephens, E.B.;  
18  
19 Tour, J.M. *Macromol.* **1993**, 26, 2420-2427; (c) Ozaki, J.; Ito, M.; Fukazawa,  
20  
21 H.; Yamanobe, T.; Hanaya, M.; Oya, A. *J. Anal. Appl. Pyrol.* **2006**, 77, 56-  
22  
23 62). Although we do not wish to be drawn on undue speculation, the low  
24  
25 carbon analysis is at least consistent with formation of such thermoset  
26  
27 materials during thermal analysis.  
28  
29  
30  
31
- 32 99. Gaussian 09, Revision A.02, Frisch, M. J.; Trucks, G. W.; Schlegel, H. B.;  
33  
34 Scuseria, G. E.; Robb, M. A.; Cheeseman, J. R.; Scalmani, G.; Barone, V.;  
35  
36 Mennucci, B.; Petersson, G. A.; Nakatsuji, H.; Caricato, M.; Li, X.; Hratchian,  
37  
38 H. P.; Izmaylov, A. F.; Bloino, J.; Zheng, G.; Sonnenberg, J. L.; Hada, M.;  
39  
40 Ehara, M.; Toyota, K.; Fukuda, R.; Hasegawa, J.; Ishida, M.; Nakajima, T.;  
41  
42 Honda, Y.; Kitao, O.; Nakai, H.; Vreven, T.; Montgomery, Jr., J. A.; Peralta,  
43  
44 J. E.; Ogliaro, F.; Bearpark, M.; Heyd, J. J.; Brothers, E.; Kudin, K. N.;  
45  
46 Staroverov, V. N.; Kobayashi, R.; Normand, J.; Raghavachari, K.; Rendell,  
47  
48 A.; Burant, J. C.; Iyengar, S. S.; Tomasi, J.; Cossi, M.; Rega, N.; Millam, J.  
49  
50 M.; Klene, M.; Knox, J. E.; Cross, J. B.; Bakken, V.; Adamo, C.; Jaramillo, J.;  
51  
52 Gomperts, R.; Stratmann, R. E.; Yazyev, O.; Austin, A. J.; Cammi, R.;  
53  
54 Pomelli, C.; Ochterski, J. W.; Martin, R. L.; Morokuma, K.; Zakrzewski, V.  
55  
56 G.; Voth, G. A.; Salvador, P.; Dannenberg, J. J.; Dapprich, S.; Daniels, A.  
57  
58 D.; Farkas, O.; Foresman, J. B.; Ortiz, J. V.; Cioslowski, J.; Fox, D. J.  
59  
60 *Gaussian, Inc.*, Wallingford CT, 2009.

100. (a) Becke, A.D. *J. Chem. Phys.* **1993**, 98, 5648-5652. (b) Lee, C.; Yang, W.; Parr, R.G. *Phys. Rev. B* **1988**, 37, 785-789.
101. (a) Petersson, G.A.; Al-Laham, M.A. *J. Chem. Phys.* **1991**, 94, 6081-6090. (b) Petersson, G.A.; Bennett, A.; Tensfeldt, T.G.; Al-Laham, M.A.; Shirley, W.A.; Mantzaris, J. *J. Chem. Phys.* **1988**, 89, 2193-2218.
102. (a) V. Barone, M. Cossi, *J. Phys. Chem. A* **1998**, 102, 1995-2001. (b) M. Cossi, N. Rega, G. Scalmani, V. Barone, *J. Comput. Chem.* **2003**, 24, 669-681.
103. GaussView 5.0, Dennington, R. D.; Keith, T. A.; Millam, J. M. *Gaussian, Inc.*, Wallingford CT, 2008.
104. O'Boyle, N. M., Tenderholt, A. L.; Langner, K. M. *J. Comp. Chem.* **2008**, 29, 839-845.
105. Ditchfield, R. *Mol. Phys.* **1974**, 27, 789-807; Rohling, C. M.; Allen, L. C.; Ditchfield, R. *Chem. Phys.* **1984**, 87, 9-15; Wolinski, K.; Hinton, J. F.; Pulay, P. *J. Am. Chem. Soc.* **1990**, 112, 8251-8260.

FOR TABLE OF CONTENTS USE ONLY



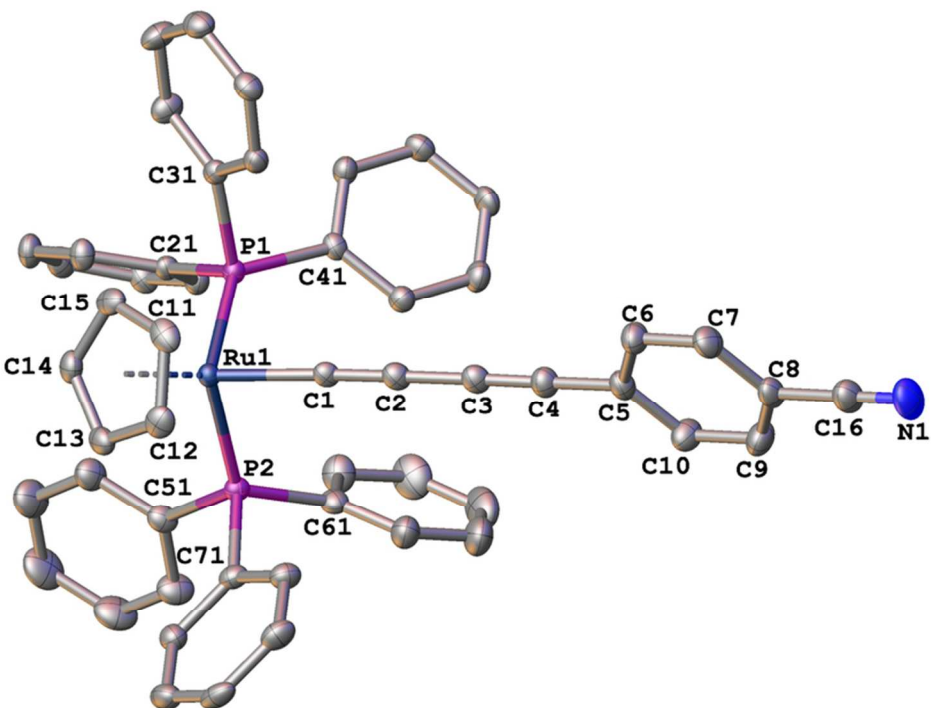


Fig.1 Molecular structure of 4a showing the atom labeling scheme. In this and all subsequent plots thermal ellipsoids are drawn at 50% probability level, H-atoms and solvent molecules are omitted for clarity.  
73x53mm (300 x 300 DPI)

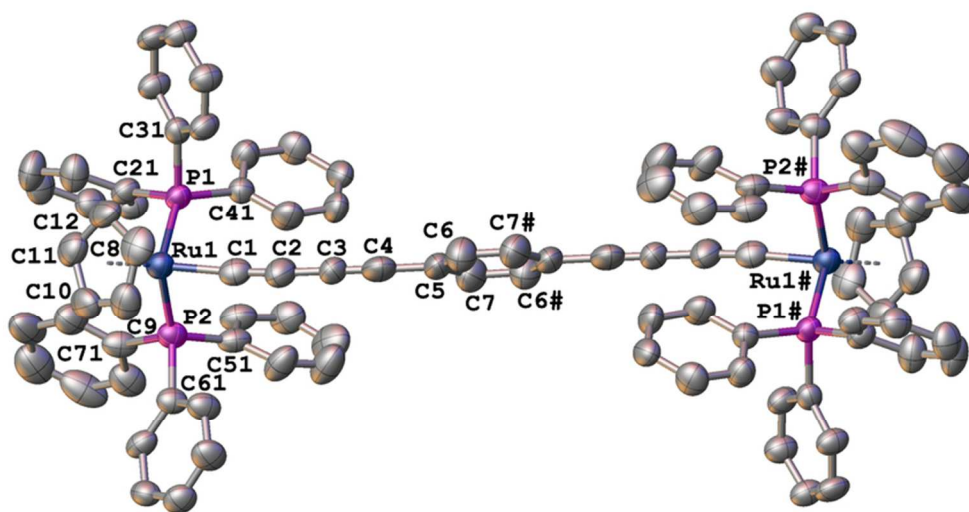


Fig. 2. A plot of a molecule of 5. The molecule is located in the center of symmetry.  
73x53mm (300 x 300 DPI)

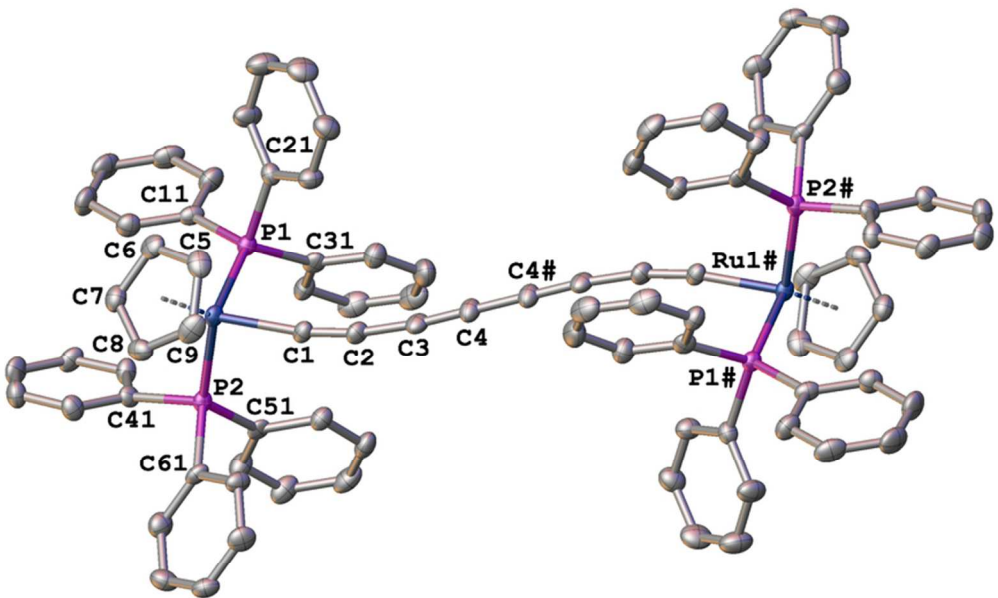


Fig. 3. A plot of a molecule of 6. The molecule is located in the center of symmetry.  
73x53mm (300 x 300 DPI)

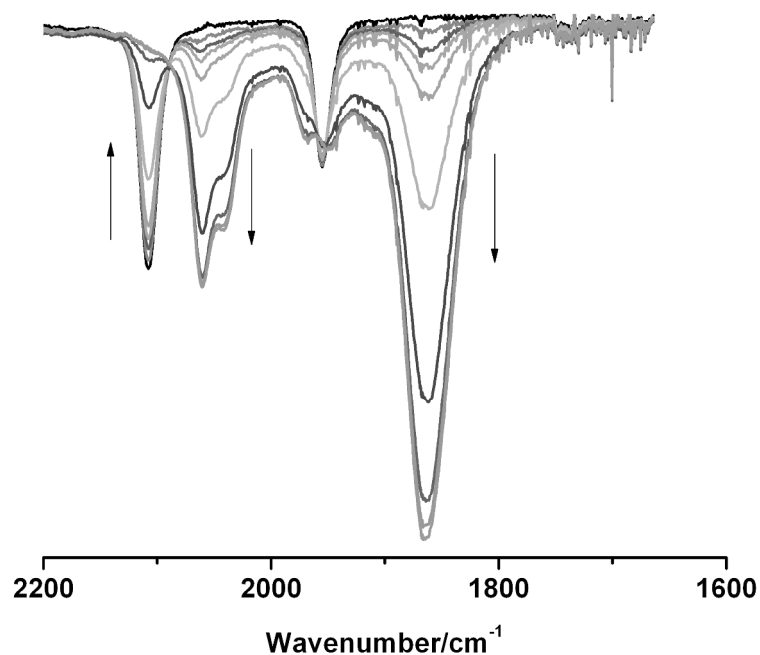


Fig. 4. The IR spectra collected in a spectroelectrochemical cell during oxidation of 6 (0.1 M NBu<sub>4</sub>PF<sub>6</sub> / CH<sub>2</sub>Cl<sub>2</sub>).  
273x207mm (300 x 300 DPI)



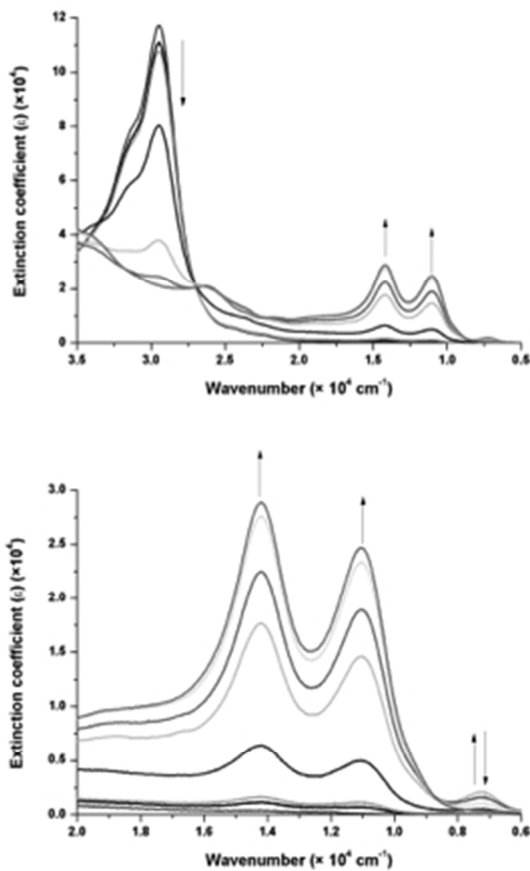
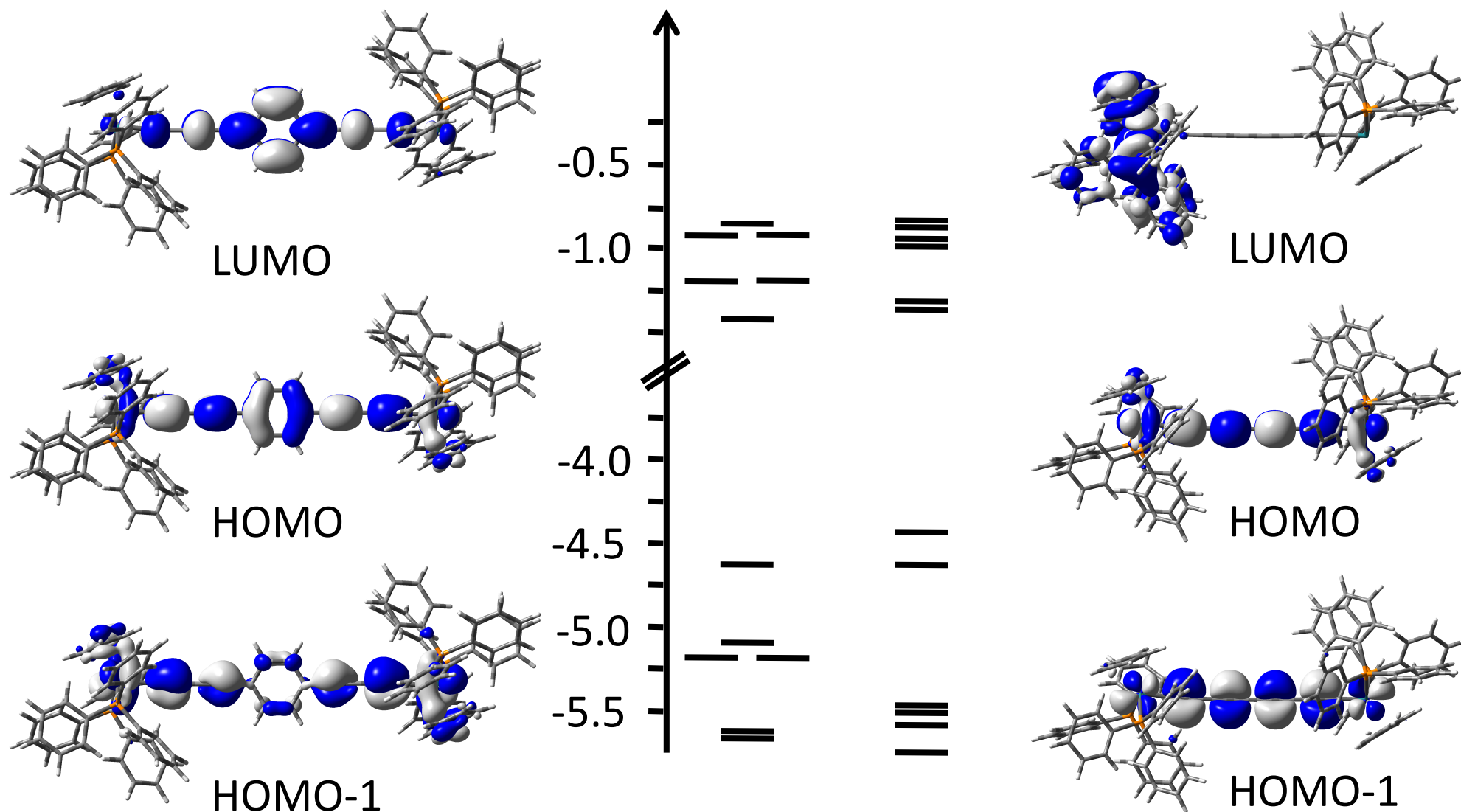
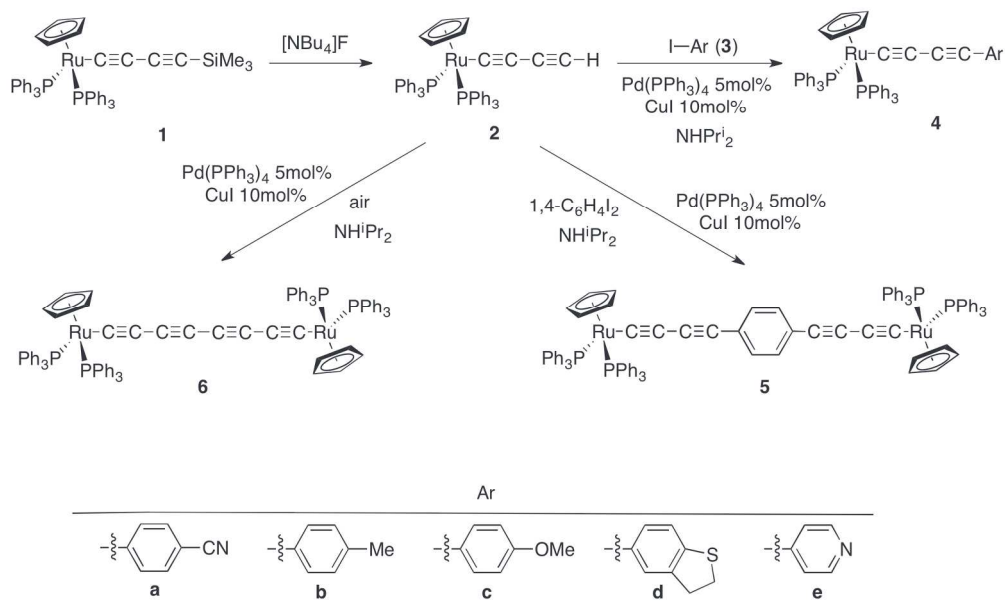
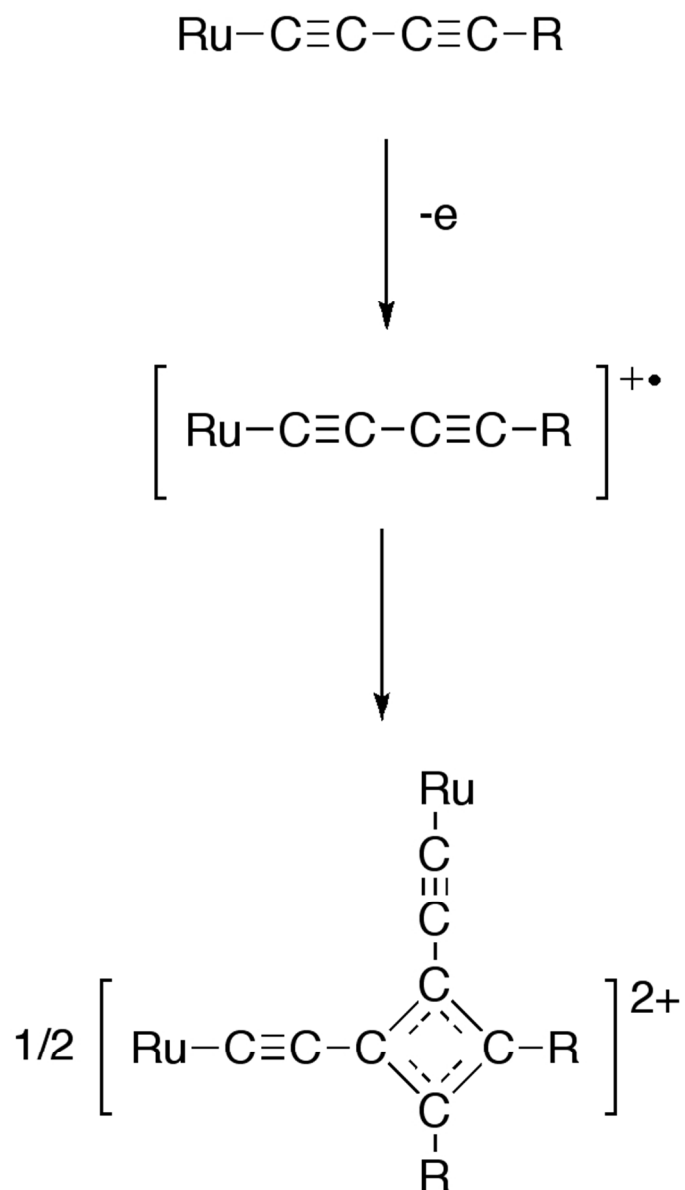


Fig 5. The UV-Vis-NIR spectra collected in a spectroelectrochemical cell during oxidation of 6 (0.1 M NBu<sub>4</sub>PF<sub>6</sub> / CH<sub>2</sub>Cl<sub>2</sub>).  
114x166mm (72 x 72 DPI)

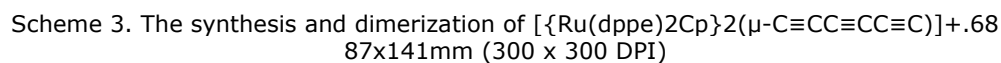


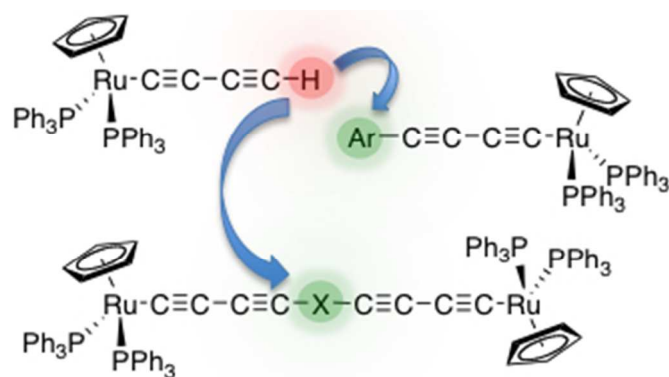


188x112mm (300 x 300 DPI)



Scheme 2. A general oxidation and dimerization process for a Ru-C≡C-C≡C-R complex [Ru = Ru(PP)Cp' where PP = (PPh<sub>3</sub>)<sub>2</sub> or dppe, Cp' = Cp or Cp\*; R = aryl or -(C≡C)<sub>n</sub>-Ru].  
53x93mm (300 x 300 DPI)





For Table of Contents Use Only  
118x65mm (72 x 72 DPI)